NSWC TR 86-26

DTIC FILE COPY

GALVANIC CORROSION OF Al-7075-T6 AND STEEL-4340 COUPLED TO BRASS QQ-B-626,360 AND Al-7075-T6 COUPLED TO STEEL-4130 AND STEEL-4340: EXPOSURE TO AQUEOUS NaCl AND SALT-FOG ENVIRONMENTS

AD-A179 121

BY J. F. McINTYRE S. M. HOOVER K. A. MUSSELMAN

RESEARCH AND TECHNOLOGY DEPARTMENT

30 JUNE 1986

DTIC ELECTE APR 15 1987 S D

Approved for public release; distribution is unlimited.

NAVAL SURFACE WEAPONS CENTER

Dahlgren, Virginia 22448-5000 • Silver Spring, Maryland 20903-5000

Best Available Copy

87 4 15 102

UNCLASSIFIED
SECURITY CLASSIFICATION OF THIS PAGE

REPORT DOCUMENTATION PAGE

1a. REPORT SECURITY CLASSIFICATION Unclassified	1b RESTRICTIVE MARKINGS
2a. SECURITY CLASSIFICATION AUTHORITY	3. DISTRIBUTION/AVAILABILITY OF REPORT Approved for public release; distribution is unlimited.
2b. DECLASSIFICATION/DOWNGRADING SCHEDULE	
4. PERFORMING ORGANIZATION REPORT NUMBER(S) NSWC TR 86-26	5. MONITORING ORGANIZATION REPORT NUMBER(S)
6a. NAME OF PERFORMING ORGANIZATION Naval Surface Weapons Center 6b. OFFICE SYMBOL (If applicable) R33	7a. NAME OF MONITORING ORGANIZATION
6c. ADDRESS (City, State, and ZIP Code) 10901 New Hampshire Ave Silver Spring, MD 20903-5000	7b. ADDRESS (City, State, and ZIP Code)
8a. NAME OF FUNDING/SPONSORING ORGANIZATION 8b. OFFICE SYMBOL (If applicable)	9. PROCUREMENT INSTRUMENT IDENTIFICATION NUMBER
8c. ADDRESS (City, State, and ZIP Code)	10. SOURCE OF FUNDING NUMBERS PROGRAM ELEMENT NO. / PROJECT NO. / TASK NO / WORK UNIT ACCESSION NO.
11. TITLE (Include Security Classification) Galvanic Corrosion of Al-7075-T6 and Steel-4340 Coupled to Brass QQ-B-626, 360 and Al-7075-T6 Coupled to Steel-4130 and Steel-4340; Exposure to Aqueous NaCl and Salt-Fog Environments	
12. PERSONAL AUTHOR(S) McIntyre, J.F. (R33), Hoover, S.M. (R32), and Musselman, K.A. (R35)	
13a. TYPE OF REPORT Technical Review 13b. TIME COVERED FROM 6/85 TO 12/85	14. DATE OF REPORT (Year, Month, Day) 86/6/30 15. PAGE COUNT 59
16. SUPPLEMENTARY NOTATION	

17. COSATI CODES		
FIELD	GROUP	SUB-GROUP
11	06	01

18. SUBJECT TERMS (Continue on reverse if necessary and identify by block number)
Galvanic Corrosion, Polarization Resistance, Cathode, Anode, Salt-Fog, Cathodic Polarization, Zero-Impedance Ammeter, Galvanic Current Density, aluminum alloys

19. ABSTRACT (Continue on reverse if necessary and identify by block number)
For this investigation, laboratory studies on the corrosion behavior of four galvanic couples is discussed; the four couples include: Al-7075-T6/Brass QQ-B-626, 360, Al-7075-T6/Steel-4340, Al-7075-T6/Steel-4130, and Steel-4340/Brass QQ-B-626, 360. Test samples were exposed to aqueous 3.5% NaCl and to a salt-fog environment. A measurement of the galvanic current generated for each couple tested was used to determine the magnitude of galvanic interaction. Results indicated that the corrosion rate of Al-7075-T6 was significantly accelerated when galvanically coupled to brass or the steel samples. In addition, it was discovered that Steel-4130 and Steel-4340 corroded when coupled to Al-7075-T6, however, at a reduced rate when compared to the uncoupled steel samples. In contrast, brass samples revealed no signs of corrosion when coupled to either Al-7075-T6 or Steel-4340. For the Steel-4340/Brass galvanic couple, it was found that the corrosion rate of Steel-4340 was significantly increased while the brass sample remained unaffected. In addition to the discussion of experimental results, a theoretical treatment relating galvanic currents to observed corrosion rates are presented for each of the four couples.

20. DISTRIBUTION/AVAILABILITY OF ABSTRACT ☒ UNCLASSIFIED/UNLIMITED ☐ SAME AS RPT. ☐ DTIC USERS	21. ABSTRACT SECURITY CLASSIFICATION UNCLASSIFIED
22a. NAME OF RESPONSIBLE INDIVIDUAL J. F. McIntyre	22b TELEPHONE (Include Area Code) (202) 394-4115 22c. OFFICE SYMBOL R33

DD FORM 1473, 84 MAR 83 APR edition may be used until exhausted. All other editions are obsolete

SECURITY CLASSIFICATION OF THIS PAGE

☆U.S. Government Printing Office: 1985—630-012

0102-LF-014-6602

UNCLASSIFIED

Keywords:

FOREWORD

Dissimilar metal corrosion is a persistent problem faced by the fleet because of the need to utilize a variety of different metals to construct complex structures as dictated by the increasing number of mechanical, metallurgical, and economical requirements. In light of these facts, it is imperative that laboratory testing be conducted in order to recognize potential galvanic problems in advance. This report is a compilation of introductory galvanic corrosion data obtained for several important metallic couples exposed to aggressive NaCl environments.

The potential risks of galvanic corrosion are particularly significant to NAVY concerns, especially when dissimilar metals are employed in critical weapon systems; therefore, this preliminary research was initiated to predict and establish the galvanic corrosion behavior associated with the following metals: Al-7075-T6, Steel-4130, Steel 4340, and Brass QQ-B-626,360. The research activities reported herewithin are a first in a series of reports to be published on the galvanic corrosion behavior of critical materials essential to the integrity of selected weapon sytems.

Approved by:

Jack R. Dixon

JACK R. DIXON, Head
Materials Division

Accesion For
NTIS CRA&I ☑
DTIC TAB ☐
U. announced ☐
Justification .....
By .....
Distribution /
Availability Codes
Dist | Avail and / or Special
A-1

CONTENTS

ILLUSTRATIONS

ILLUSTRATIONS (Cont.)

TABLES

Chapter 1

INTRODUCTION

The corrosion of metals can be described as a step-wise interaction of events involving chemical, electrical, and physical processes occurring at the interface between a metal and its environment. Common to all corrosion mechanisms is the occurrence of two distinct reactions involving oxidation and reduction processes. In general, these reactions take place at specific anodic and cathodic sites on the metal surface. Metal atoms are oxidized to metal ions at anodic sites liberating electrons. These electrons migrate, i.e. electrical interaction, to cathodic sites where they are consumed by the species being reduced.

A potentially dangerous situation may occur when two metals with different electrochemical reactivities are physically joined. Corrosion involving dissimilar metals in contact is known as galvanic or bimetallic corrosion. Most galvanic corrosion is unwanted and often unexpected. For example, a ship constructed of nickel alloy and steel rivets becomes unseaworthy because the steel rivets are active and preferentially corrode at a high rate. The hot-water tank in your home can be troublesome if a steel tank is connected to copper tubing.

Dissimilar metal corrosion is a persistent problem faced by design engineers because of the need to utilize a variety of different metals to construct complex structures as dictated by the large number of mechanical, metallurgical, and economical requirements. Care must be exercised when making material selection, however, proper testing of candidate materials should recognize problem areas in advance.

When two dissimilar metals are placed in the same environment, a potential difference develops. When electrical contact is made between the two metals, a current flows; the direction of current flow is dependent on the metal's electrochemical activity in that environment and, in general, can be predicted using the measured corrosion potentials of the uncoupled metals. A metal exhibiting a more active corrosion potential, i.e., the more negative value, should act as the anode and the direction of current flow will be from the anode to the cathode, i.e., the metal with the more positive or noble corrosion potential. Corrosion of the more active metal will be significantly increased and attack at the more noble metal will be decreased, as compared to their uncoupled behavior. In order to prevent galvanic corrosion, the potential difference between two metals in contact must be made small or one of the metals must be electrically insulated.

Initially the standard reduction potential table was used to predict which metal of an electrically or physically connected couple would act as the anode or the cathode. This approach turns out to be dangerous and often incorrect.

These potentials are measured against the standard hydrogen electrode in aqueous solutions of unit activity of the metal of interest and this is not representative of typically encountered environments; in addition, the behavior of alloys cannot be predicted using this table. A number of investigators have assembled and constructed tables that predict the galvanic corrosion tendencies of commonly used metals and alloys. One such galvanic series was constructed by The International Nickel Company at Harbor Island, N.C., and is based on potential measurements and corrosion tests in seawater. This series is reproduced in Table 1 where the relative positions of the metals are used rather than their potentials and brackets are used to designate those metals which are similar in base composition and behavior. When metals within a given bracket are coupled, there is little chance of significant galvanic corrosion occurring. This table and others like it only apply to the specific environment in which the test data is collected and the position of a metal or alloy or groups of metals or alloys may change as the environment changes. Ideally it would be advantageous to construct galvanic tables for all possible combinations of metal and/or alloy couples and their environments. Obviously this would prove to be quite tedious and impractical; therefore, individual tests need to be made on the metal or alloy of choice in the environment of interest.

In order to effectively estimate the rate of galvanic corrosion, the current produced by galvanic action must be monitored. A large sustained galvanic current suggests that significant corrosion will take place. Equally feasible is the occurrence of an initially high current which rapidly decreased with time because of the accumulation of adherent corrosion products on the anode. In this case, a low rate of galvanic corrosion is likely. This observation strongly indicates that galvanic couples must be monitored over an extended period of time. Mansfeld and Kenkel (1) and Baboian (2) review the experimental techniques which can be used to follow galvanic corrosion currents with time.

Another factor which influences the extent to which galvanic corrosion occurs involves the polarizability of the metal cathode of the couple. A highly efficient cathode will produce high cathodic currents serving to drive the anodic reaction, i.e., an increase in the anodic dissolution rate. For example, titanium is a highly noble metal even when exposed to seawater and when coupled to a less corrosion resistant metal or alloy, one would intuitively expect that rapid attack would occur; this is not the case, the corrosion rate is low because titanium is a poor catalyst for the cathodic reduction of oxygen.

Galvanic corrosion occurs in the immediate vicinity of the couple where the galvanic currents are the strongest. As a general rule of thumb, the severity of galvanic corrosion decreases as the distance from the coupled area increases. Unfortunately galvanic influence in local areas can produce catastrophic results e.g., sudden failure of joined parts, leading to the loss of structural integrity.

The cathode-to-anode area ratio of coupled metals strongly influences the rate of galvanic corrosion and requires careful consideration. For example, if two steel panels are joined by copper rivets and exposed to seawater, the steel panels will corrode, however, the bond between the two panels will remain intact. Copper is more noble than steel and, therefore, acts as the cathode. The generated anodic current at the steel anode is distributed over a large area

TABLE 1. GALVANIC SERIES

↑ Noble or cathodic	Platinum
	Gold
	Graphite
	Titanium
	Silver
	Chlorimet 3 (62 Ni, 18 Cr, 18 Mo)
	Hastelloy C (62 Ni, 17 Cr, 15 Mo)
	18-8 Mo stainless steel (passive)
	18-8 stainless steel (passive)
	Chromium stainless steel 11-30% Cr (passive)
	Inconel (passive) (80 Ni, 13 Cr, 7 Fe)
	Nickel (passive)
	Silver solder
	Monel (70 Ni, 30 Cu)
	Cupronickels (60-90 Cu, 40-10 Ni)
	Bronzes (Cu-Sn)
	Copper
	Brasses (Cu-Zn)
	Chlorimet 2 (66 Ni, 32 Mo, 1 Fe)
	Hastelloy B (60 Ni, 30 Mo, 6 Fe, 1 Mn)
	Inconel (active)
	Nickel (active)
	Tin
	Lead
	Lead-tin solders
	18-8 Mo stainless steel (active)
	18-8 stainless steel (active)
	Ni-resist (high Ni cast iron)
	Chromium stainless steel, 13% Cr (active)
	Cast iron
	Steel or iron
	2024 aluminum (4.5 Cu, 1.5 Mg, 0.6 Mn)
Active or anodic ↓	Cadmium
	Commercially pure aluminum (1100)
	Zinc
	Magnesium and magnesium alloys

and, as a result, small anodic current densities are produced. This small anodic current density translates into small corrosion rates. On the other hand, connecting two copper panels together with steel rivets causes rapid deterioration of the steel rivets because of the reduced anode area which must now sustain large current densities, thus, significant corrosion occurs and the bond between the copper plates fail.

Reboul (3) and Mansfeld et al. (4) provide excellent reviews on the galvanic corrosion behavior of aluminum coupled to a large number of metals and alloys exposed to seawater and tap water. Mansfeld et al. (4) constructed a table rank-ordering 95 galvanic couples, where one metal of the couple was an aluminum alloy; a general ranking can be given in decreasing order of galvanic current generated by each of the following metals when coupled to an aluminum alloy: $Ag > Cu > 4130$ steel $\gg$ stainless steel $\approx Ni >$ Inconel 718 $\gg$ Ti-6Al-4V $\approx$ Haynes 188 $> Sn > Cd$. Mansfeld et al. (4) summarizes the behavior of aluminum alloys as follows; Al 1100 is only compatible with Cd, Al 6061 only with Al 7075, 2024, 2219, and Al 7075 is only compatible with other aluminum alloys and Zn. In general, it is almost impossible to couple aluminum and its alloys to any other metal and expose it to seawater without protecting the structure by painting or insulating the dissimilar metals from one another.

In summary, the magnitude of galvanic corrosion is dependent on the potential difference between dissimilar metals, the kinetics of the individual anodic and cathodic reactions, the nature of the environment, i.e., highly conductive solutions will produce large currents, and the cathode-to-anode area ratio. The measurement of corrosion potentials can only be used to predict the direction of galvanic current flow and in no way can it be used to predict the extent of galvanic corrosion; continuous monitoring of galvanic currents provides the only reliable and accurate method of assessing the galvanic effect.

Chapter 2

EXPERIMENTAL

MATERIALS

Four alloys were investigated for this galvanic study. They include: Aluminum 7075-T6, Steel-4340, Steel-4130, and Brass QQ-B-626, 360. The following couples were investigated: Al-7075/Steel-4340, Al-7075/Brass, Al-7075/Steel-4130, and Steel-4340/Brass. The Brass, Al-7075, and Steel-4340 samples were machined into cylindrical shapes having a uniform height of 0.625" with three diameters: 0.3125", 0.375", and o.4375" and, because of availability, disk shaped Steel 4130 samples were used in place of cylinders. In an attempt to maintain identical conditions for the Al-7075/Steel couple, Al-7075-T6 samples were also machined into disks. Lead wires were attached to these samples followed by cold-mounting in an acrylic polymer; the disk samples had the following diameters: 0.750", 0.45", and 0.375". Prior to testing, the samples were wet-polished from 180 through 600 grit SiC finish. All specimens were degreased in acetone followed by a methanol rinse prior to exposure. Solutions were prepared from reagent grade chemicals and distilled water. Corrosion and galvanic couple potentials are reported with respect to the Saturated Calomel Electrode (SCE).

TEST METHODS

The electrochemical corrosion test cells used in this study can be seen in Figure 1. Galvanic corrosion was studied by monitoring the current generated between the galvanic couples using a Princeton Applied Research Model 351 Corrosion Test System, where the model 351 system used a zero-impedance ammeter to measure the galvanic corrosion current. Galvanic data is presented in a plot of galvanic current against time, generally one hour was sufficient to reach a steady-state current value. Galvanic current was monitored immediately upon immersion for one hour and again after 24 hours; in addition, the galvanic current was monitored for periods longer than 24 hours for several of the couples.

Corrosion rates for each of the coupled metal samples were individually determined immediately following galvanic current measurement. The PAR 351 System was used to make all corrosion rate measurements and, for this study, the polarization resistance (Rp) technique was used to determine the sample's corrosion rate. The Rp technique was selected over weight-loss determinations because of the unique advantages inherent to this technique. These benefits include the following: measurements can be made in short times without removing the sample from its environment; there is minimal material destruction, the corrosion rate can be monitored against time, and small rates of corrosion can be measured. Briefly, Rp measurements involve the application of a controlled-potential scan over a small range, typically $\pm$ 5mV with respect to

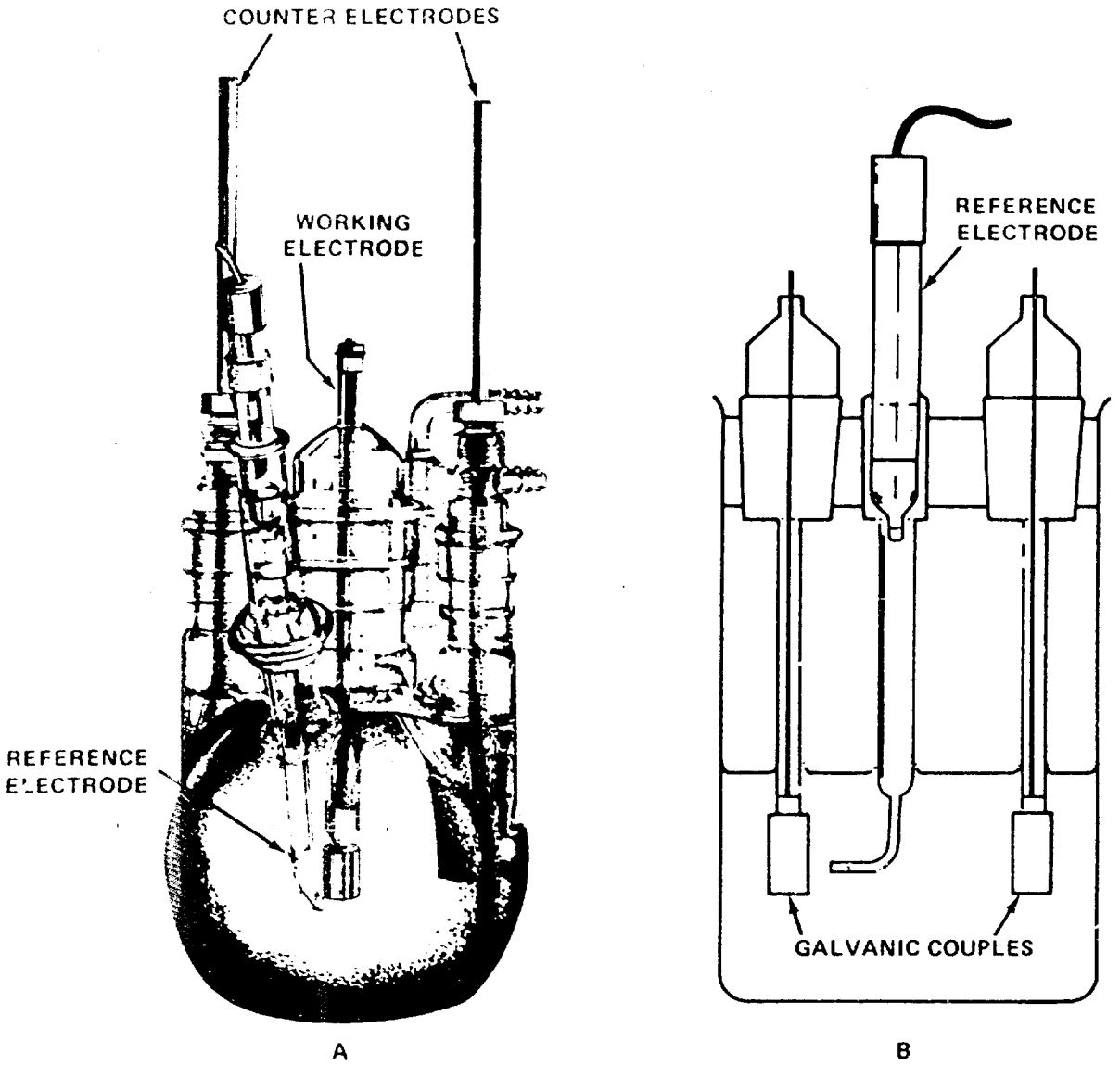

FIGURE 1. ELECTROCHEMICAL CORROSION TESTING CELLS
A- ELECTROCHEMICAL CELL FOR R_p MEASUREMENT
B- GALVANIC CURRENT MEASUREMENT CELL

the corrosion potential. In this potential range the applied potential and current are linearly related to a close approximation. The resultant current is plotted against the applied potential and the slope of the straight line at the potential where the current passes through zero is equal to the polarization resistance (See Figure 2). Measured Rp values are inversely proportional to the corrosion current. See equation [1]:

$$i_{corr} = \frac{1}{Rp} \quad \frac{\beta a \beta c}{2.303(\beta a + \beta c)} \tag{1}$$

where i_{corr} is the corrosion current, βa is the anodic Tafel constant, and βc is the cathodic Tafel constant.

Cathodic polarization curves were obtained using a potentiodynamic technique. All samples were equilibrated in a 3.5% NaCl for 1 hour prior to measurement. The cathodic scan, at a rate of 0.5 mV/sec, was started at the corrosion potential, Ecorr, and scanned in the negative direction to a final value of -1.350 V (SCE). For Al-7075-T6 samples, a anodic polarization scan was started at Ecorr and scanned to more positive potentials, i.e., + 110mV.

Galvanic couples and the individual uncoupled metals were exposed to a salt-fog environment according to ASTM standard B-368 and Mil-S-810. Each sample was cold-mounted in an acrylic polymer and placed in the salt-fog chamber at an angle of 45 degrees and continuously exposed to a 3.5% NaCl fog at 95°C for 96 hours. Galvanic coupling was accomplished by external connection of lead wires attached to the anode and cathode materials. Photographs were obtained prior to exposure. See Figures 3 and 4. Subsequently, photographs were taken immediately after removal from the salt-fog chamber and after the removal of corrosion products. Corrosion products were removed from aluminum surfaces with concentrated HNO_3 followed by a water rinse and further cleansing using a rubber eraser. Adherent corrosion products on steel surfaces were removed with concentrated HCl followed by rinsing with liberal amounts of distilled water and additional cleaning with an eraser. Brass samples were easily cleaned using an eraser.

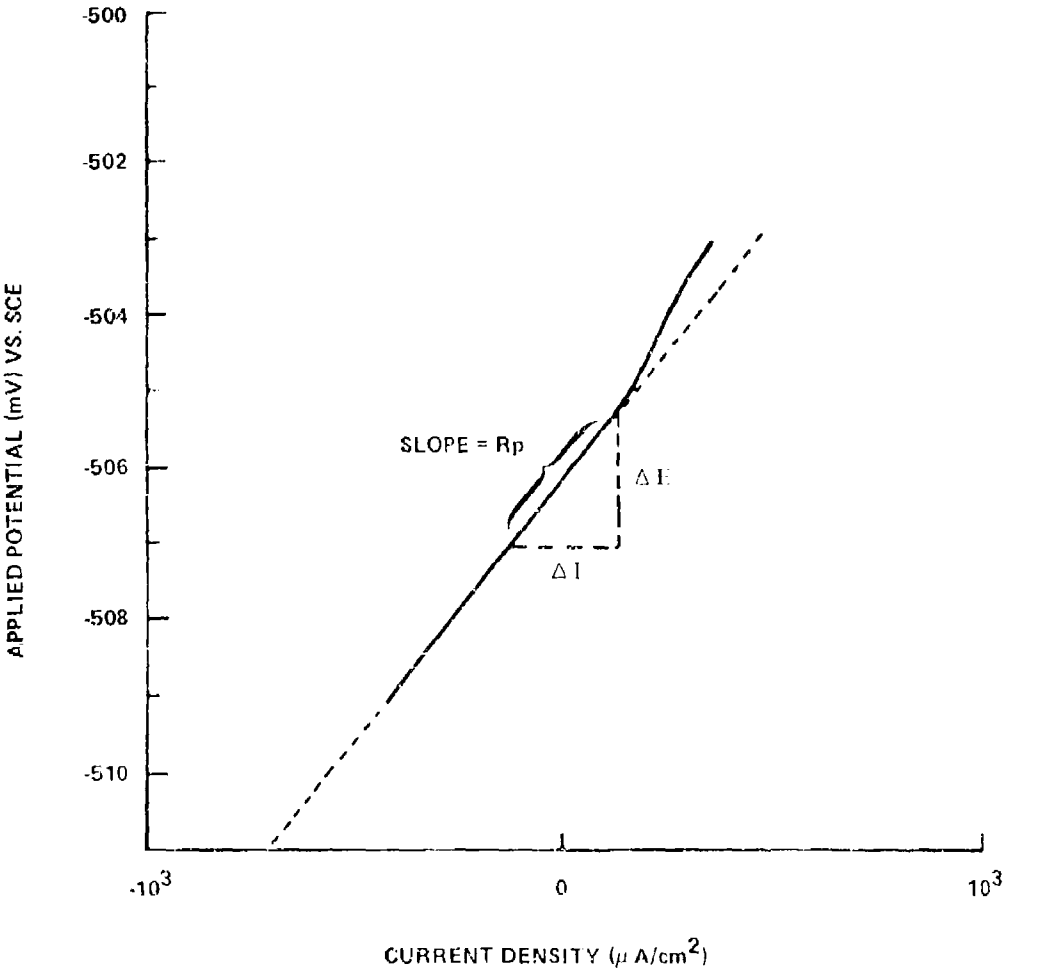

FIGURE 2. POLARIZATION RESISTANCE PLOT

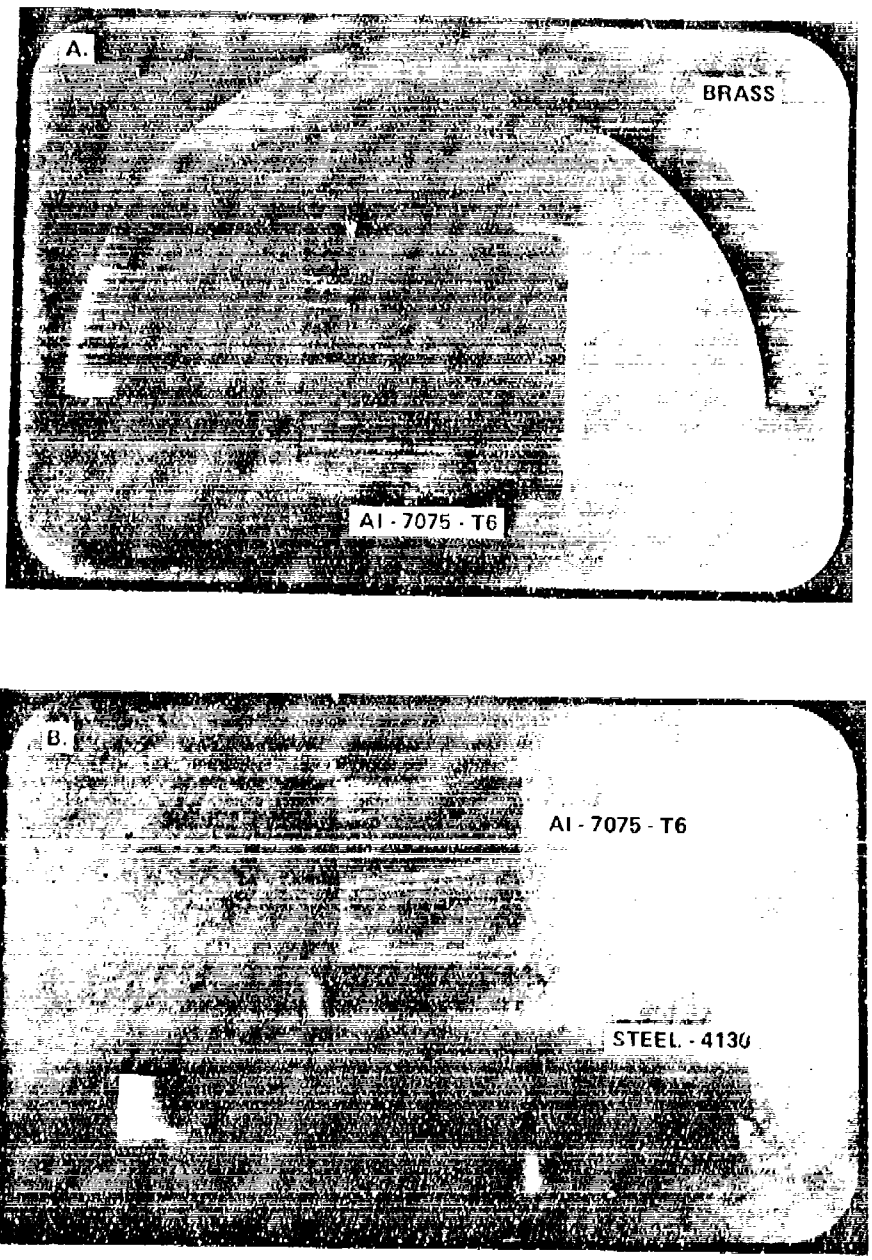

FIGURE 3. PHOTOGRAPHS OF GALVANIC COUPLES PRIOR TO SALT - FOG EXPOSURE
A - Al-7075-T6/BRASS COUPLE
B - Al-7075-T6/ST-4130 COUPLE

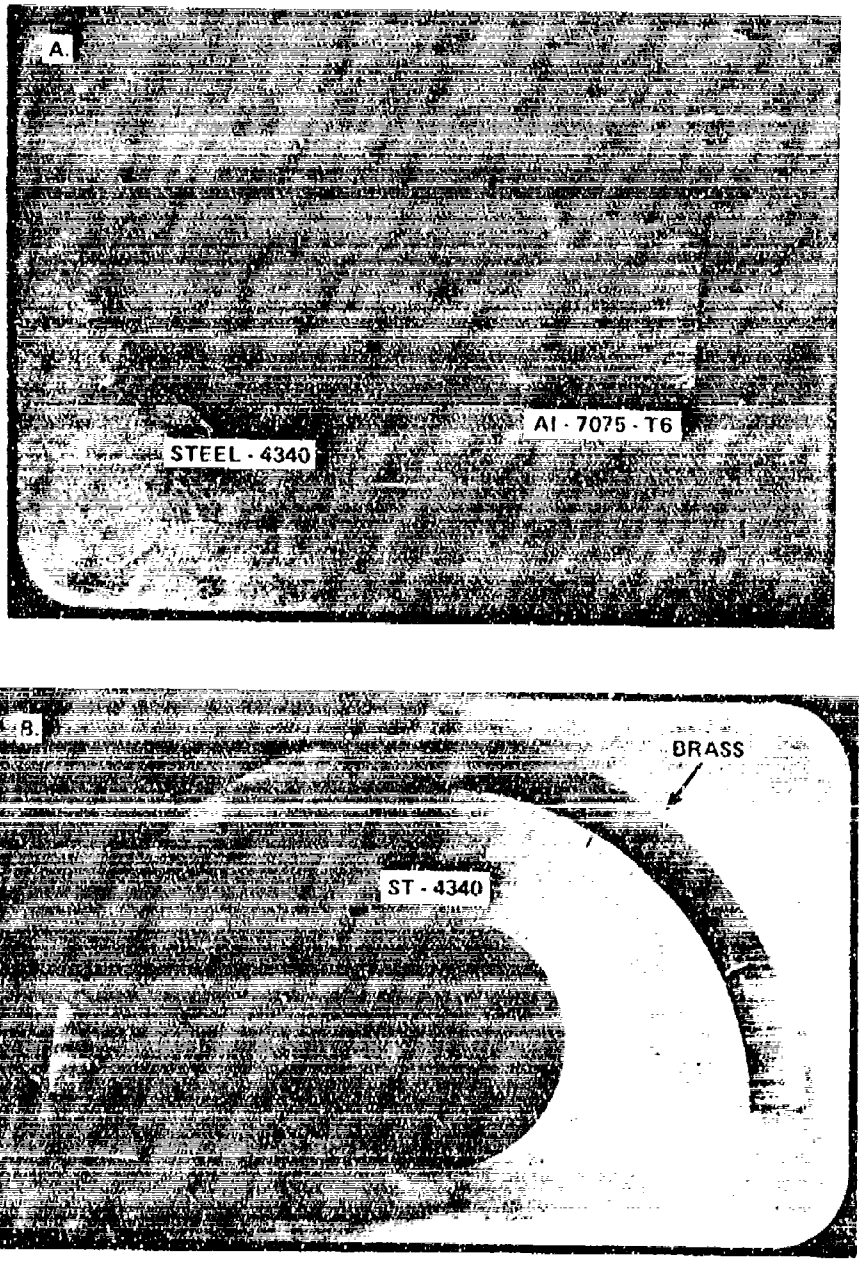

FIGURE 4. PHOTOGRAPHS OF GALVANIC COUPLES PRIOR TO SALT - FOG EXPOSURE
A - Al-7075/ST-4340 COUPLE
B - ST-4340/BRASS COUPLE

CHAPTER 3

RESULTS AND DISCUSSION

CORROSION RATES OF UNCOUPLED SAMPLES

Corrosion rate data for uncoupled metals exposes to 3.5% NaCl, obtained using the polarization resistance technique, can be seen in Table 2. Results revealed that Al7075-T6 had the lowest corrosion rate, i.e. highest Rp value, followed by Brass QQ-B-626, 360, Steel-4130, and Steel-4340. The lower corrosion rate for Al7075 can be attributed to the propensity of aluminum to corrode by pitting, i.e. localized attack; consequently, the uniform corrosion rate is much lower than observed for brass and the low-alloy steels exposed to this environment.

GALVANIC CURRENT MEASUREMENTS

Typical galvanic current/time plots can be seen in Figures 5 thru 8. Figure 5 gives results obtained for an Al7075/Brass couple exposed to 3.5% NaCl for 24 hours. The steady galvanic current density was approximately 15 $\mu A/cm^2$ (galvanic current densities are calculated by using the area of the anode, e.g., the area of Al-7075 is used for the Al-7075/Brass couple). A typical plot obtained for an Al-7075/St-4340 couple. Figure 6, gives a steady galvanic current density of 14.3 $\mu A/cm^2$ after about 23 hours of immersion. Results for a St-4340/Brass couple gave a steady galvanic current density of about 11.6 $\mu A/cm^2$ after 24 hours. See Figure 7. Lastly, the Al-7075/St-4130 couple gave a steady galvanic current density after 24 hours of about 20 $\mu A/cm^2$. See Figure 8.

Table 3 summarizes the measured galvanic currents for each of the tested couples. For couples of equal geometric surface area, the highest galvanic current density was obtained for the Al7075/St-4130 couple followed by Al-7075/Brass, Al-7075/St-4340, and the St-4340/Brass couple. For comparison, a reported literature value for an Al-7075-T76/Steel-4130 couple exposed to 3.5% NaCl for 24 hours was 25$\mu A/cm^2$ (1). This value is not too different from the galvanic current density generated by the Al-7075-T6/St-4130 couple in this experiment. The larger galvanic current density reported for the Al-7075/St-4130 couple is surprising when compared to the Al-7075/St-4340 and Al-7075/Brass couples. St-4340 should be more corrosion resistant, i.e., more noble, than St-4130 because of higher Mo content and the addition of Ni to St-4340. In fact, the corrosion potential, Ecorr, in Table 4, for St-4340 was more noble by about 45 mV suggesting that higher galvanic currents might indeed be generated when St-4340 is coupled to Al-7075. On the other hand, brass with the most noble Ecorr value suggests that even higher galvanic currents might be expected when brass is coupled to Al-7075. Therefore, the relative nobility of the cathode material in the galvanic couple does not determine the overall

TABLE 2. CORROSION RATES, REPORTED AS POLARIZATION RESISTANCE VALUES, FOR UNCOUPLED METALS EXPOSED TO 3.5% NaCl

SAMPLE	TIME (hrs)	Rp(ohms.cm^2)
AL-7075-T6	24	9440
BRASS	21	4530
STEEL-4130	23	2160
STEEL-4340	24	2094

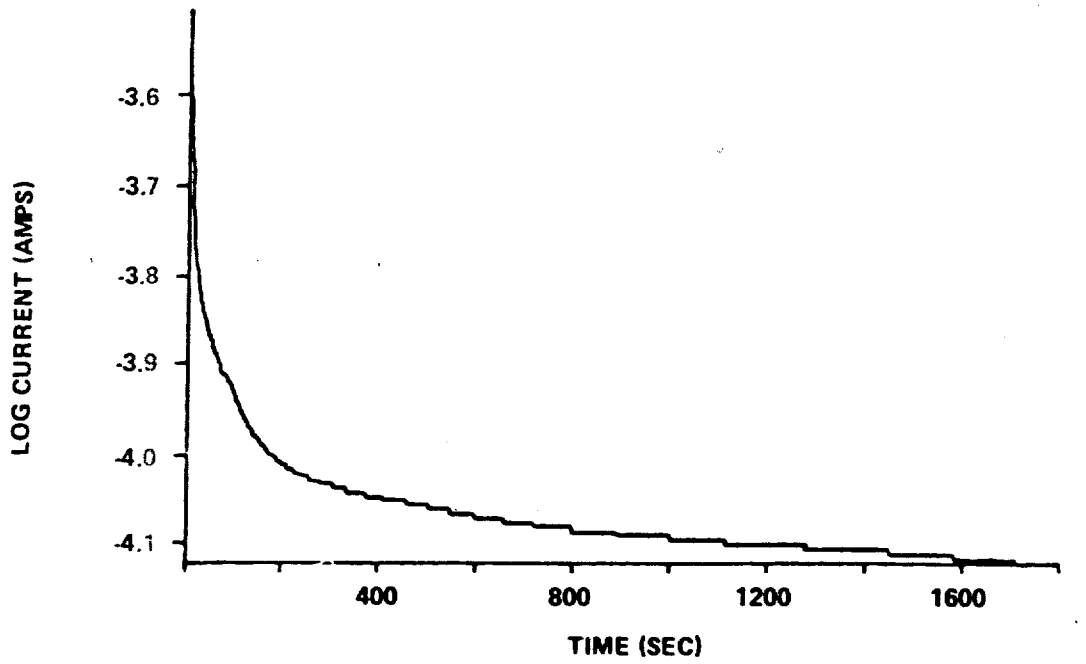

FIGURE 5. PLOT OF GALVANIC CURRENT AGAINST TIME FOR Al - 7075 - T6/BRASS COUPLE EXPOSED TO 3.5% NaCl FOR 24 HOURS

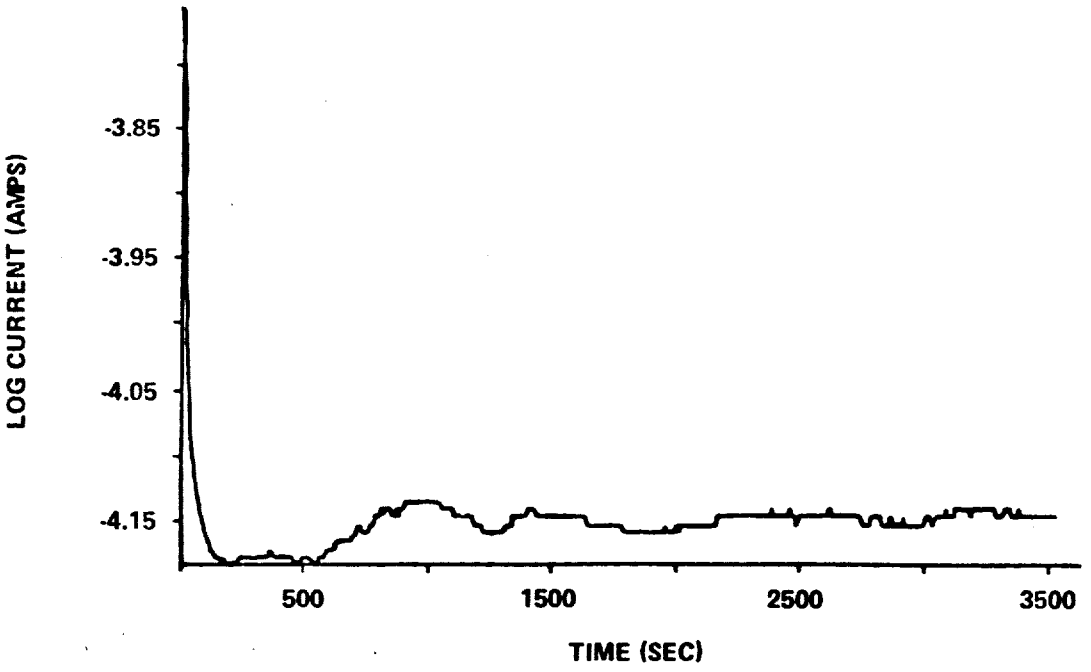

FIGURE 6. PLOT OF GALVANIC CURRENT AGAINST TIME FOR Al - 7075 -T6/STEEL - 4340 COUPLE EXPOSED TO 3.5% NaCl FOR 24 HOURS

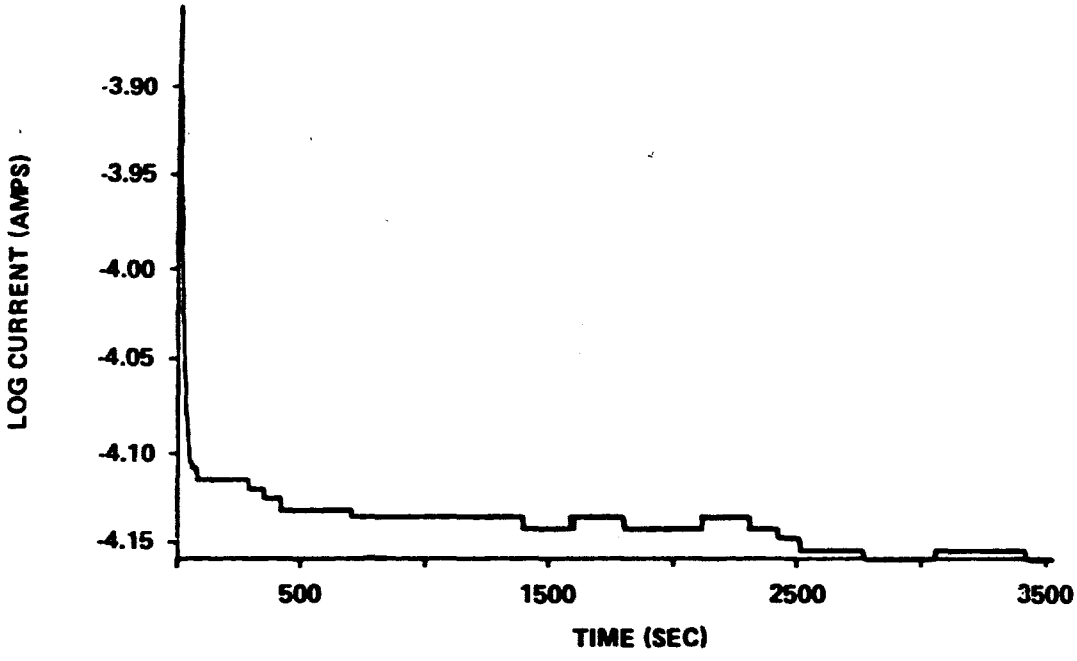

FIGURE 7. PLOT OF GALVANIC CURRENT AGAINST TIME FOR STEEL - 4340/BRASS COUPLE EXPOSED TO 3.5% NaCl FOR 24 HOURS

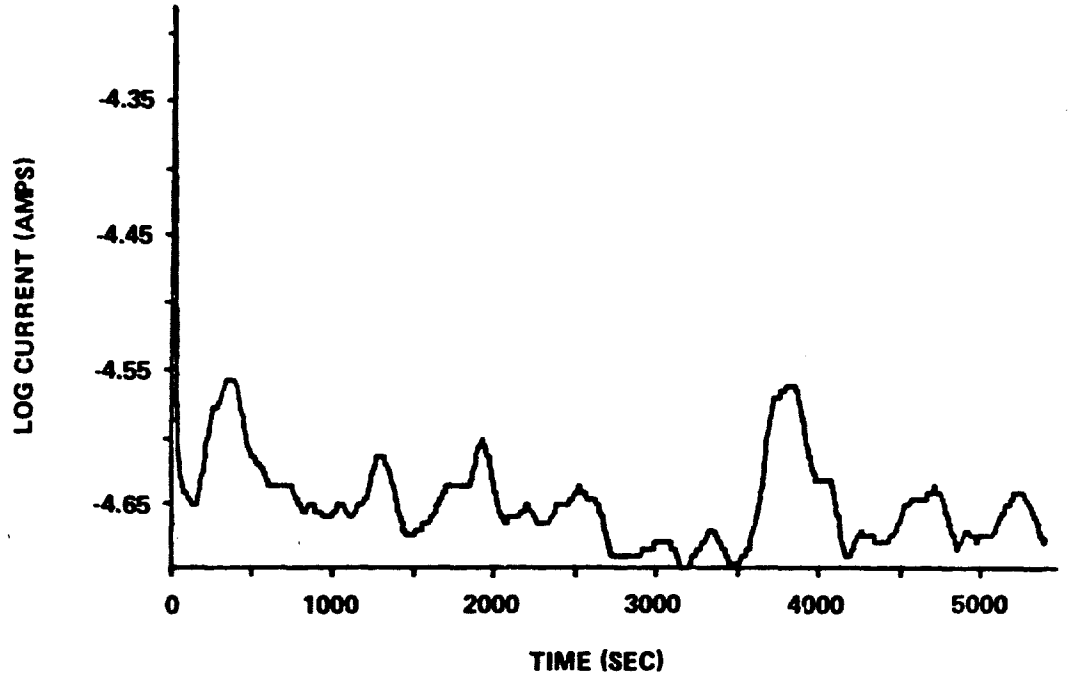

FIGURE 8. PLOT OF GALVANIC CURRENT AGAINST TIME FOR Al - 7075 - T6/STEEL - 4130 COUPLE EXPOSED TO 3.5% NaCl FOR 20 HOURS

TABLE 3. GALVANIC CURRENT DENSITIES FOR DIFFERENT CATHODE-TO-ANODE AREA RATIOS FOR VARIOUS TIMES OF EXPOSURE TO 3.5% NaCl

COUPLE	AREA RATIO	ANODE AREA	TIME(hrs)	i_{gal} ($\mu A/cm^2$)
Al-7075/St-4130	LC	0.62	24	30.32
	E	1.03	20	20.19
	SC	2.83	24	14.88
	SC	2.83	46	8.38
Al-7075/Brass	LC	4.79	19	19.70
	E	4.96	24	15.06
	SC	7.38	24	8.78
Al-7075/St-4340	LC	4.92	24	17.32
	E	4.96	23	14.27
	SC	7.34	24	8.34
St-4340/Brass	LC	4.82	24	18.05
	E	7.41	20	11.47
	SC	7.38	25	8.37
	E	6.10	24	11.77
	E	6.10	42	11.52
	E	6.10	116	10.39

LC - Large Cathode Area
E - Equal Anode and Cathode Areas
SC - Small Cathode Area

TABLE 4. EQUILIBRIUM CORROSION POTENTIALS FOR UNCOUPLED SAMPLES EXPOSED TO 3.5% NaCl

SAMPLE	TIME(hrs)	Ecorr(mV)
BRASS	24	-249 ± 25
STEEL-4340	24	-641 ± 14
STEEL-4130	23	-679 ± 25
Al-7075-T6	24	-813 ± 21

strength of the galvanic current. A discussion concerning additional effects on the galvanic current will be treated later in this paper.

EFFECT OF SURFACE AREA RATIO

Cathode-to-anode area ratio effects on the generated galvanic current density is also displayed in Table 3. The important influence of the cathode-to-anode area ratio was established by changing the relative surface area of the cathode. For example, a larger brass cathode area for an Al-7075/Brass couple resulted in an increase in the galvanic current density, in Table 3, and conversely a smaller cathode area reduced the galvanic current density. This trend was observed for all of the tested couples. When an unfavorable couple cannot be prevented, it is imperative that large cathode-to-anode ratios be avoided.

CORROSION RATES FOR GALVANIC COUPLES

Corrosion rates were obtained for the individual metals of each couple immediately after galvanic current measurements were completed. See Table 5. Typical Rp plots for some of the tested samples can be seen in Figures 9 thru 11. A comparison must be made between the corrosion rates obtained for the uncoupled metals in Table 2, and the coupled metals in Table 5. In each case, the corrosion rate of the more anodic material of the couple increased compared to its' uncoupled value, i.e., a decrease in the Rp value. For example, the experimental Rp value for an uncoupled Al-7075 sample exposed to 3.5% NaCl for 24 hours was 9,440 ohms.cm^2, but a similar Al-7075 sample coupled to brass for 24 hours gave an Rp value of 3,595 ohms.cm^2, a relatively significant increase in the corrosion rate. By comparison, an uncoupled Steel-4340 gave an Rp value of 2,094 ohms.cm^2 and after being coupled to brass for 24 hours the corrosion rate decreased slightly to a value of 1,930 ohms.cm^2; the galvanic corrosion current data supported this observation, that is the lower galvanic current density generated by the Steel-4340/Brass couple as compared to the Al-7075/Brass couple suggested that a lower corrosion rate for St-4340 should be obtained. Experience predicts that the more noble metal, i.e., the cathode in a galvanic couple should exhibit a lower rate of corrosion when coupled to a more active metal, i.e., the anode (sacrificial anodes are designed to provide protection for a ship's steel hull.); this behavior was observed for one Brass/Al-7075 sample, the Rp value of 9,4000 ohms.cm^2. However, the corrosion resistance of brass in several other galvanic couples behaved similarly to the of uncoupled brass. For the Al-7075/St-4340 couple, the corrosion rate of Al-7075 increased as expected and the corrosion rate of St-4340 decreased slightly when compared to uncoupled St-4340. The corrosion rate for Al-7075 in the Al-7075/St-4130 couple also increased but, unlike St-4340 in the Al-7075/St-4340 couple, a slight increase in the corrosion rate was observed for St-4130. This increase in the corrosion rate for St-4130 would not be predicted based on the magnitude of the galvanic current density recorded for this couple; this small increase in the corrosion rate for St-4130 supports the notion that St-4130 does not behave solely as a cathode in the couple but, also, supports an anodic dissolution reaction as well. Indeed, a visual inspection of Al-7075/St-4130 couples revealed the presence of localized attack of St-4130.

TABLE 5. CORROSION RATES FOR INDIVIDUAL METALS AFTER GALVANIC COUPLING FOR 24 HOURS IN 3.5% NaCl

COUPLE	TIME (hrs)	Rp(ohms·cm^2)
Al-7075/St-4130	Al-7075	2520
	St-4130	1730
Al-7075/Brass	Al-7075	3595
	Brass	4200
Al-7075/St-4340	Al-7075	4955
	St-4340	2455
St-4340/Brass	St-4340	1930
	Brass	2480

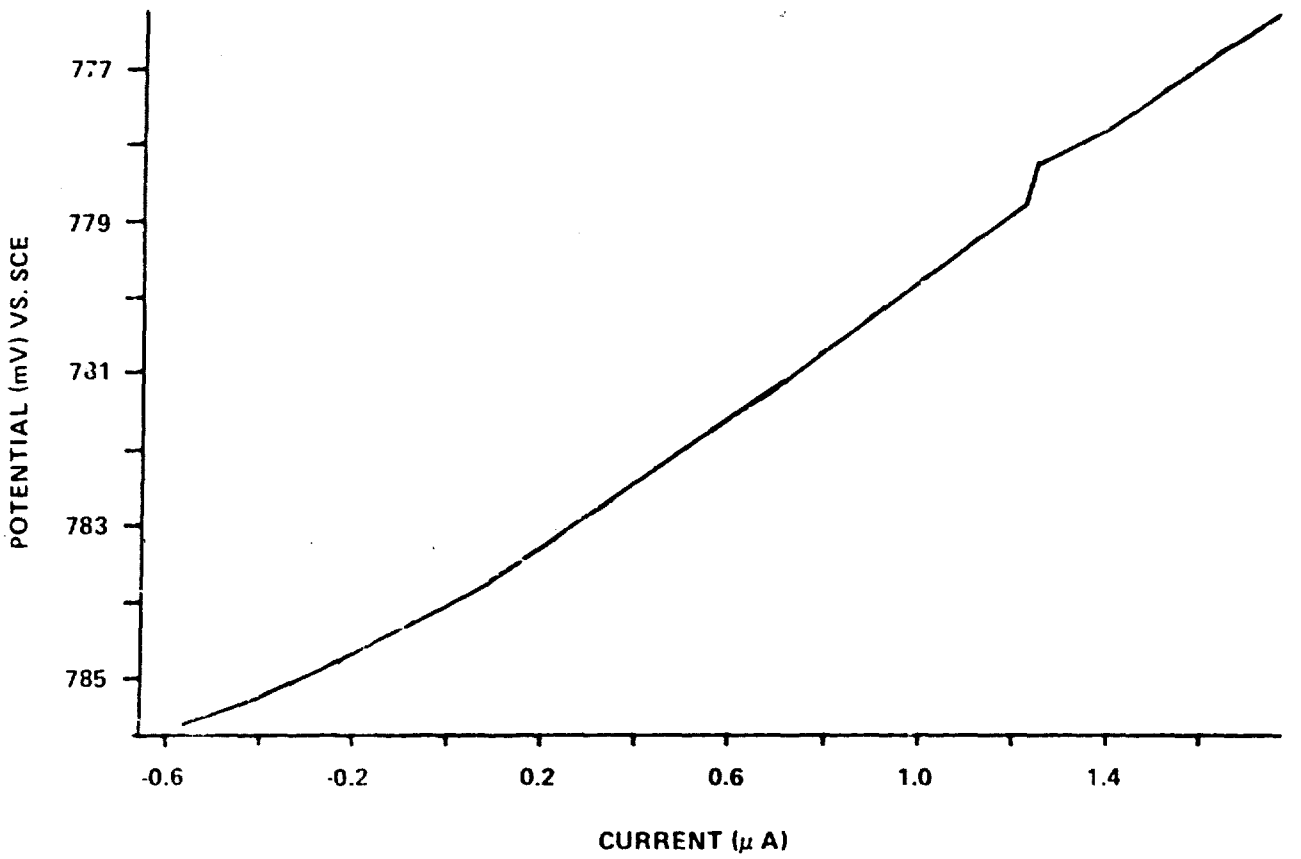

FIGURE 9. POLARIZATION RESISTANCE PLOT FOR Al-7075-T6 AFTER GALVANIC COUPLING TO STEEL - 4130, EXPOSURE TO 3.5% NaCl FOR 24 HOURS

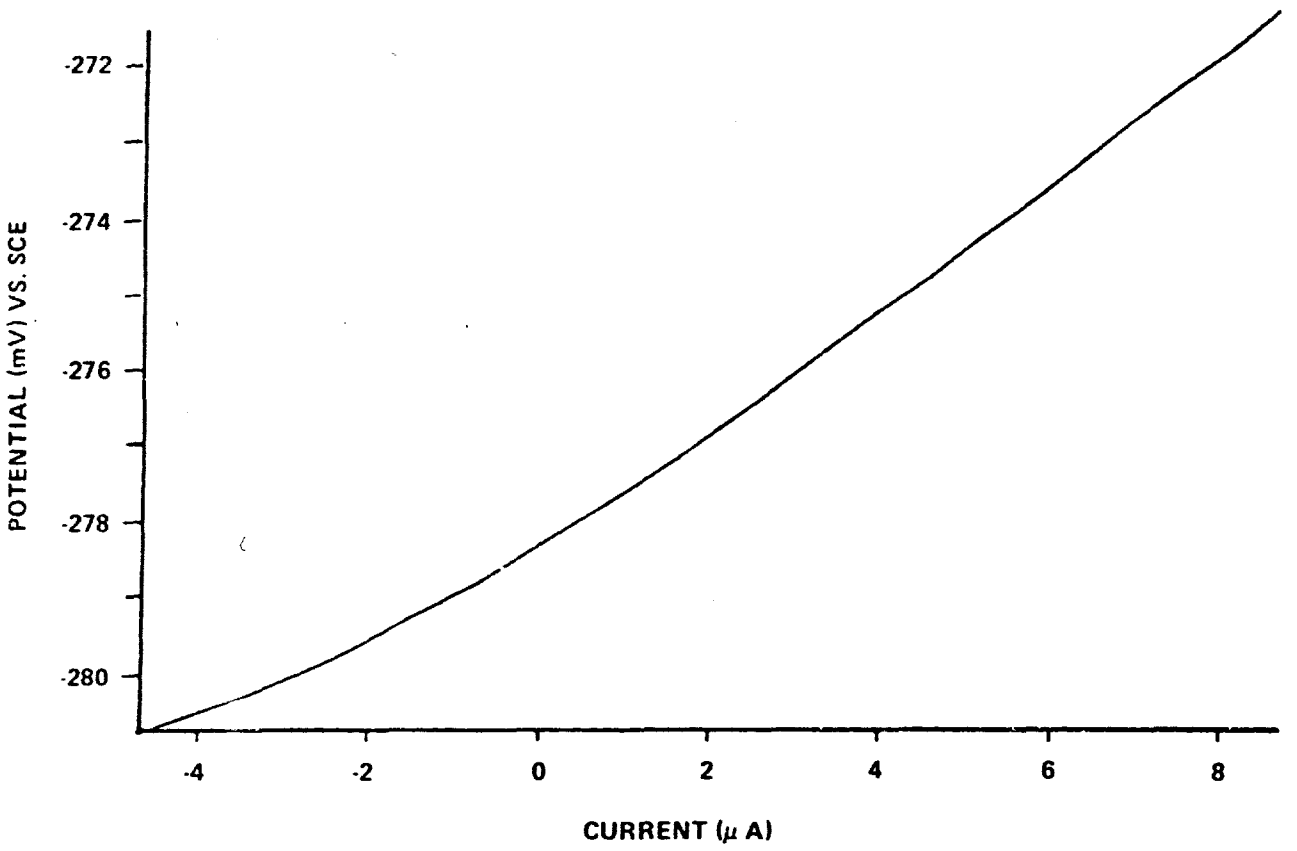

FIGURE 10. POLARIZATION RESISTANCE PLOT FOR BRASS AFTER GALVANIC COUPLING TO Al-7075-T6, EXPOSURE TO 3.5% NaCl FOR 24 HOURS

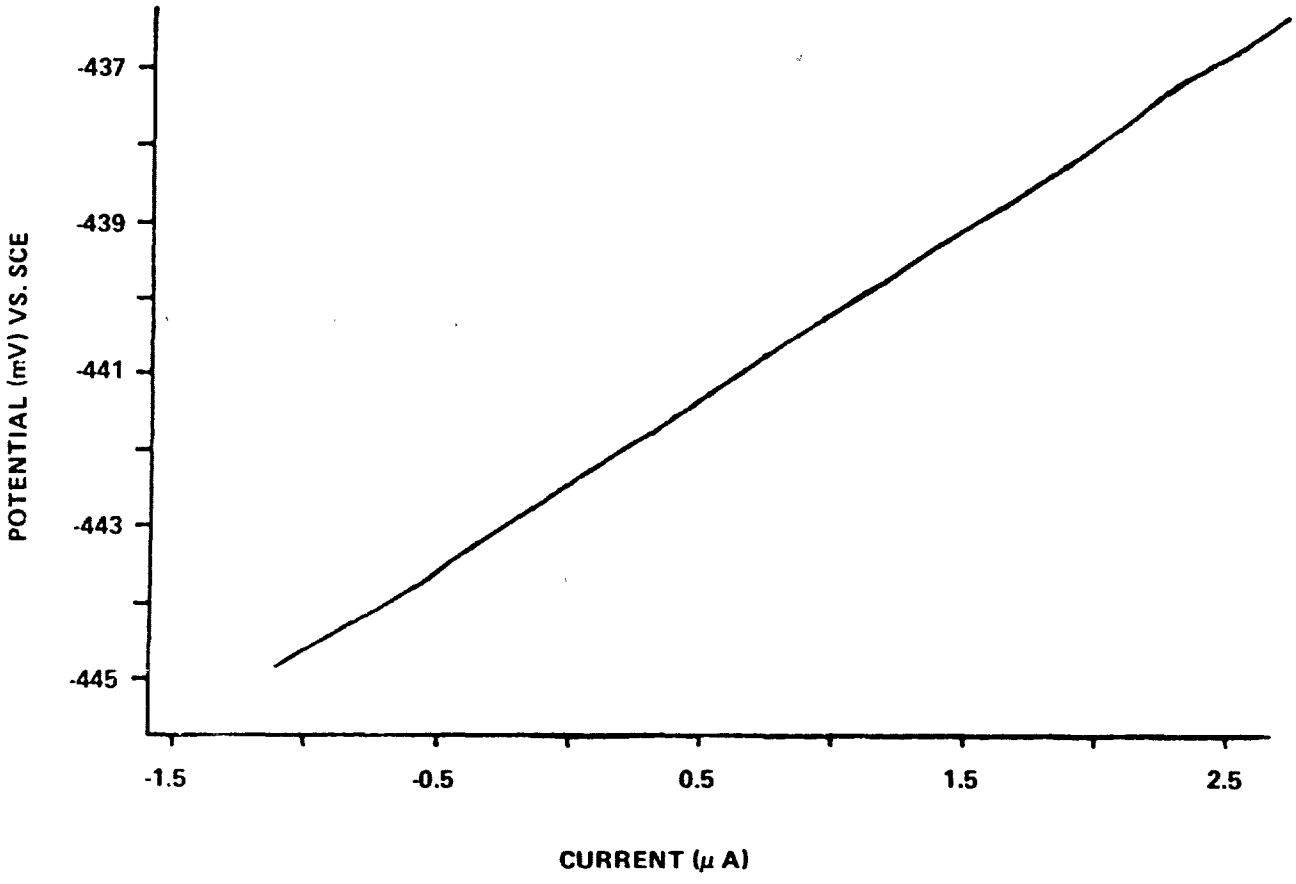

FIGURE 11. POLARIZATION RESISTANCE PLOT FOR STEEL - 4130 AFTER GALVANIC COUPLING TO Al - 7075 - T6, EXPOSURE TO 3.5% NaCl FOR 24 HOURS

CATHODIC POLARIZATION BEHAVIOR

As mentioned in the introduction, a number of factors influence the magnitude of generated galvanic currents and one such factor involves the kinetics of the cathodic reduction reaction. Cathodic behavior was studied by running polarization curves for the individual uncoupled metal samples. Representative cathodic polarization curves for the uncoupled samples exposed to 3.5% NaCl can be seen in Figure 12. Lower cathoic currents were obtained for Al-7075 than for brass, St-4340 and St-4130. This observed behavior for Al-7075 and other aluminum alloys is well documented and the lower cathodic currents can be attributed to the high electronic resistance of aluminum oxide. An insulator-like oxide will impede electron transport through the oxide, thus, effectively retarding the cathodic reduction reaction (5). These experimental results suggested that Al-7075 would not behave as a cathode when coupled to the more noble metals of brass, St-4340, and St-4130. As shown in Figure 12, the polarization curve for brass intersects the Al-7075 anodic curve at slightly higher current values than did St-4340 or St-4130, an indication that higher galvanic current densities might be expected for brass when coupled to Al-7075. Table 6 compares the initial galvanic current densities (recorded during the first hour of immersion) with the current densities obtained from the polarization curves in Figure 12 (the point of intersection of the cathodic curves of brass, St-4340, and St-4130 with the anodic curve of Al-7075); it's important to note that, although the initial galvanic current densities were close in value to the cathodic current densities, the Al-7075/St-4130 generated higher initial galvanic currents than did brass or St-4340 coupled to Al-7075. This observation might not be expected if the current value determined at the cathodic-anodic intersection is used as an estimate of the galvanic current. Experimental studies by Mansfeld and Parry (6) on the galvanic corrosion of Al-alloys coupled to Ti-6Al-4V or stainless steel 304 revealed good agreement between cathodic current densities (determined in the same manner as for this study) and initial galvanic current densities. With this in mind, higher galvanic currents might be expected for brass coupled to Al-7075 since its cathodic curve intersects the anodic curve of Al-7075 at a higher value that St-4130; however the fact that St-4130 intersects the Al-7075 anodic curve at a lower current value but actually generates larger galvanic currents further supports the idea that small but non-negligible anodic currents make contributions to the overall galvanic current for the Al-7075/St-4130 couple.

GALVANIC COUPLE EQUILIBRIUM POTENTIAL

A comparison between the corrosion potential, Ecorr, values of freely corroding uncoupled samples and the equilibrium potential, Ecouple, for coupled samples lends credence to our findings that St-4130 and perhaps St-4340 support anodic dissolution currents as well as cathodic currents. For the Al-7075/Brass couple, the Ecouple value of -765 mV was far removed from the Ecorr value of brass, an indication that brass behaves uniquely as a cathode. On the other hand, when St-4130 or St-4340 were coupled to Al-7075 their respective Ecorr values were close to Ecouple and since the cathodic curves for St-4130 and St-4340 intersected the anodic for Al-7075 close to their respective corrosion potentials, the galvanic current in this mixed-potential region could arise from both anodic and cathodic contributions. St-4130 and St-4340 can only act as cathodes when they are significantly polarized in the cathodic direction, that is, when Ecouple values are far removed from Ecorr values.

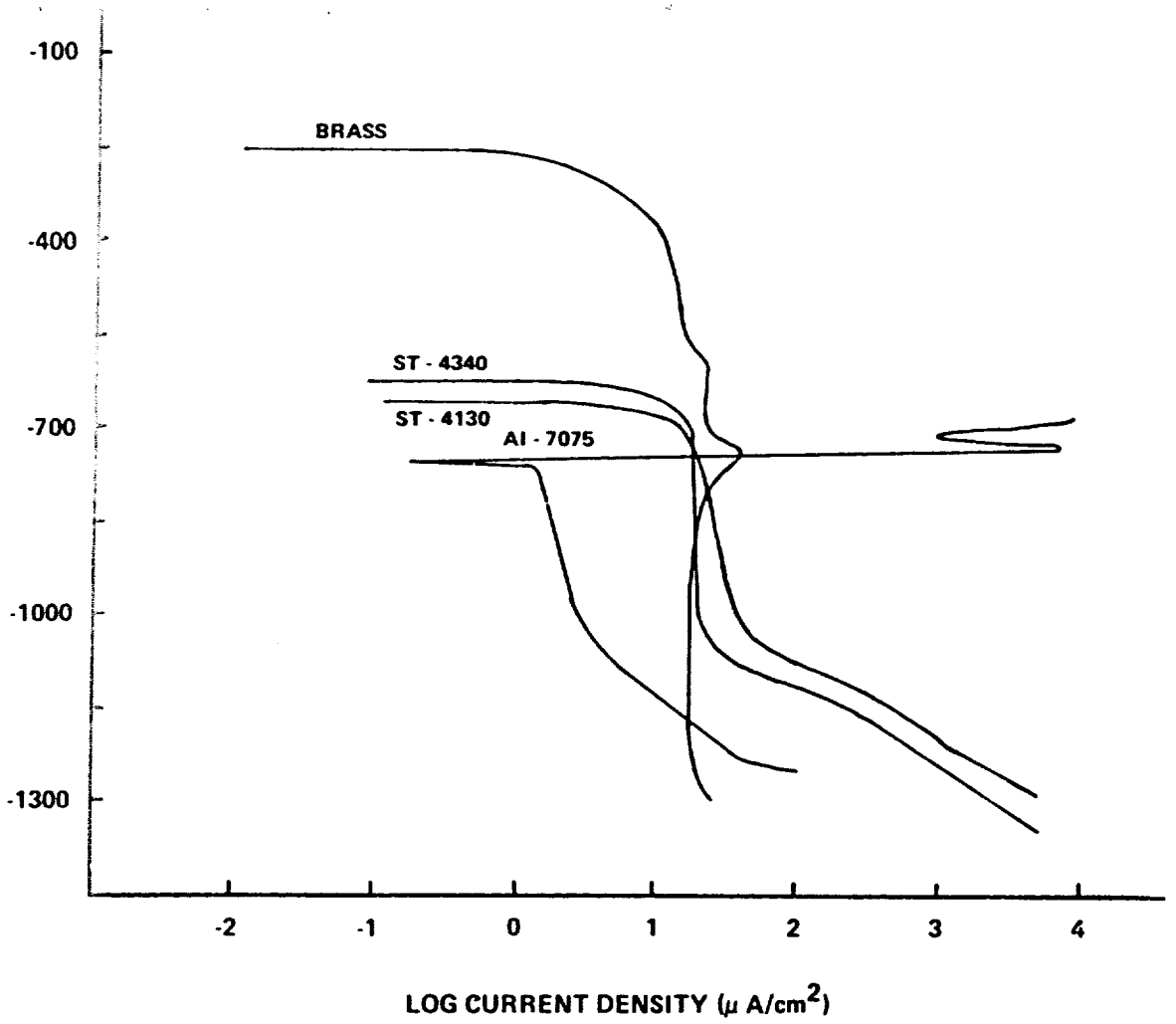

FIGURE 12. CATHODIC POLARIZATION CURVES FOR UNCOUPLED SAMPLES EXPOSED TO 3.5% NaCl

TABLE 6. COMPARISON OF THE INITIAL GALVANIC CURRENT DENSITY WITH CURRENT DENSITY AT THE INTERSECTION OF THE CATHODIC POLARIZATION CURVE OF THE CATHODE AND THE ANODIC POLARIZATION CURVE OF THE ANODE

COUPLE	INITIAL $i_{gal}(\mu A/cm^2)$	CATHODE	$i_{cath}(\mu A/cm^2)$
Al-7075/Brass	15.0	Brass	38.0
Al-7075/St-4340	16.0	St-4340	20.0
Al-7075/St-4130	17.2	St-4130	24.0
St-4340/Brass	15.4	Brass	13.0

SALT FOG TESTING

Galvanic Couple Behavior

Photographs of the Al-7075/Brass couple after salt-fog exposure can be seen in Figure 13 (for comparison, photographs of individual couples prior to exposure should be made, see Figure 3 and 4). Briefly, the aluminum surface was covered with a white loosely-adherent outer corrosion product layer and a black, tightly-adherent inner layer. Upon removal of the corrosion product layers, shown in Figure 13B, only a minute amount of uniform corrosion was detected but a number of large irregularly shaped pits were evident; also, some of the original abrasion lines from pretreatment procedures could be detected on the aluminum surface. By comparison, the brass surface was discolored by a thin film with isolated regions that were shades of blue, green, purple and brown in color. However, the brass surface beneath this discolored film was unaffected. These observations confirmed that Al-7075 was significantly attacked by coupling to brass after exposed to an aggressive environment.

Photographs of the Al-7075/Steel-4130 couple after salt-fog exposure can be seen in Figure 14. Inspection of the photograph in Figure 14A will reveal that both Al-7075 and St-4130 were significantly corroded. The aluminum surface was covered with white and black corrosion products, similar in appearance to the Al-7075 sample coupled to brass. After removal of the corrosion products from the Al-7075 sample, the underlying surface revealed that attack was predominantly of a localized nature and pits were shallow and irregularly shaped. By comparison, the Al-7075 sample coupled to brass gave much larger and somewhat deeper pits. In many areas, the original abrasion lines were easily recognizable, much more so than for Al-7075 coupled to brass or St-4340; this fact suggested that a negligible amount of uniform attack had occured. Unlike the brass cathode of the Al-7075/Brass couple, St-4130 showed signs of significant attack. The specimen was, in localized regions, covered by voluminous-tightly-adherent corrosion products. These products were yellowish-brown and black in appearance; the black corrosion product was most likely magnetite, Fe_3O_4, which formed during the incipient stages of corrosion and as oxidation of the surface continued, the formation of the loosely adherent yellowish-brown γ-Fe_2O_3 followed. Beneath these sites of corrosion product build-up were regions of deeply penetrating uniform corrosion while areas adjacent to this attack remained unaffected, as indicated by the appearance of the original lines of abrasion. See Figure 14B.

Photographs of the Al-7075/St-4340 couple after salt-fog exposure can be seen in Figure 15. Similar to the Al-7075/St-4130 couple, the St-4340 sample was also attacked and its appearance was nearly the same as St-4130 coupled to Al-7075. Voluminous corrosion products were found on the surface, that were yellowish-brown and black. See Figure 15A. As observed for the St-4130 sample, the corrosion products were strongly adherent. A fewer number of corroded regions were observed for St-4340 than for St-4130; however, the nature and appearance of the corrosive attack was identical for both steel samples, that is, uniform attack in localized areas with deep penetration while adjacent areas remained unaffected. As was observed with other galvanically coupled Al-7075 samples, the surface was covered with white and black adherent corrosion products. Beneath the corrosion products a large number of irregularly shaped pits could be seen and, also, some areas of uniform-like dissolution with

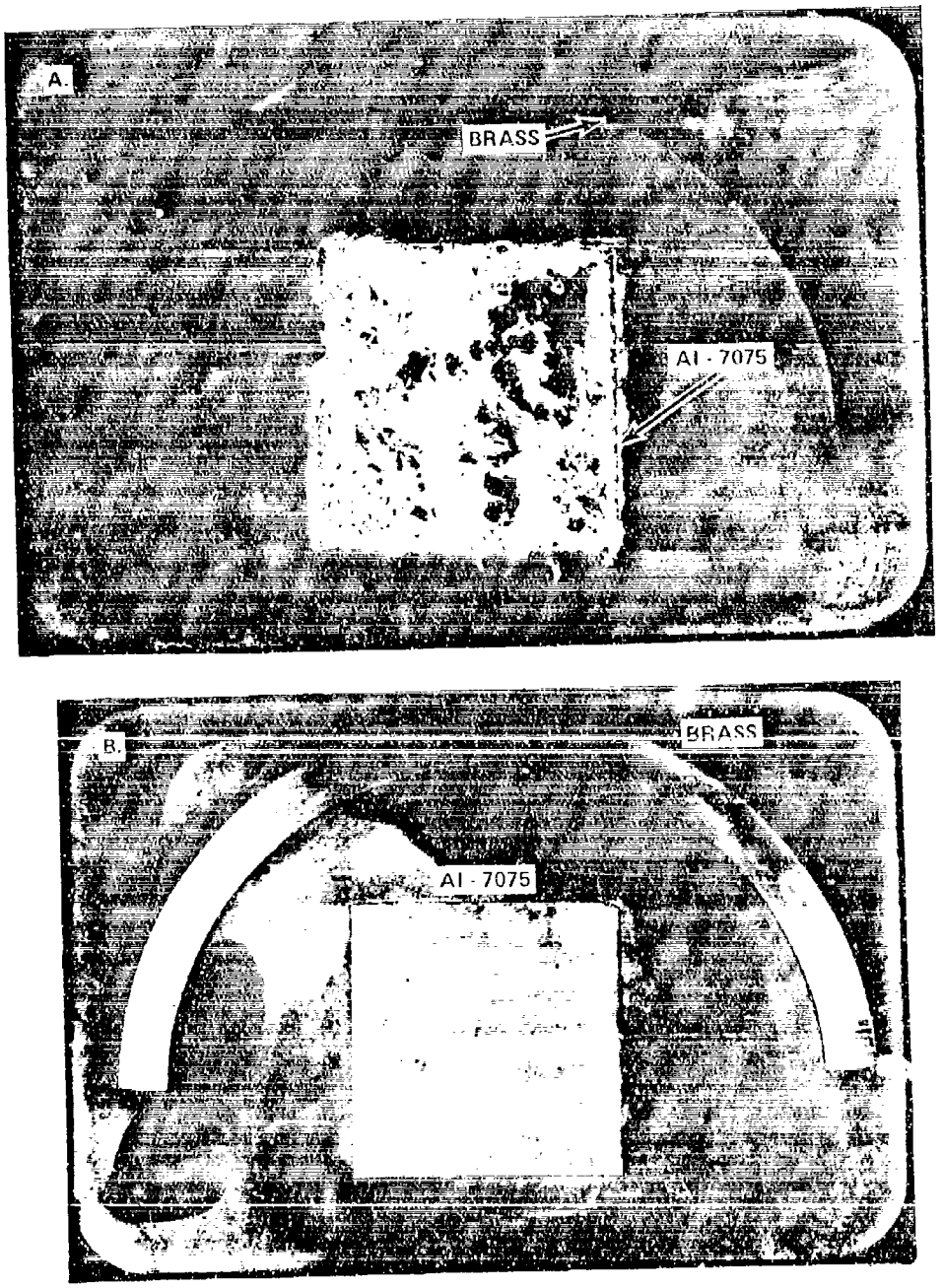

FIGURE 13. PHOTOGRAPHS OF Al 7075/BRASS GALVANIC COUPLE AFTER EXPOSURE TO A SALT - FOG ENVIRONMENT FOR 96 HOURS
A - CORROSION PRODUCTS INTACT
B - CORROSION PRODUCTS REMOVED

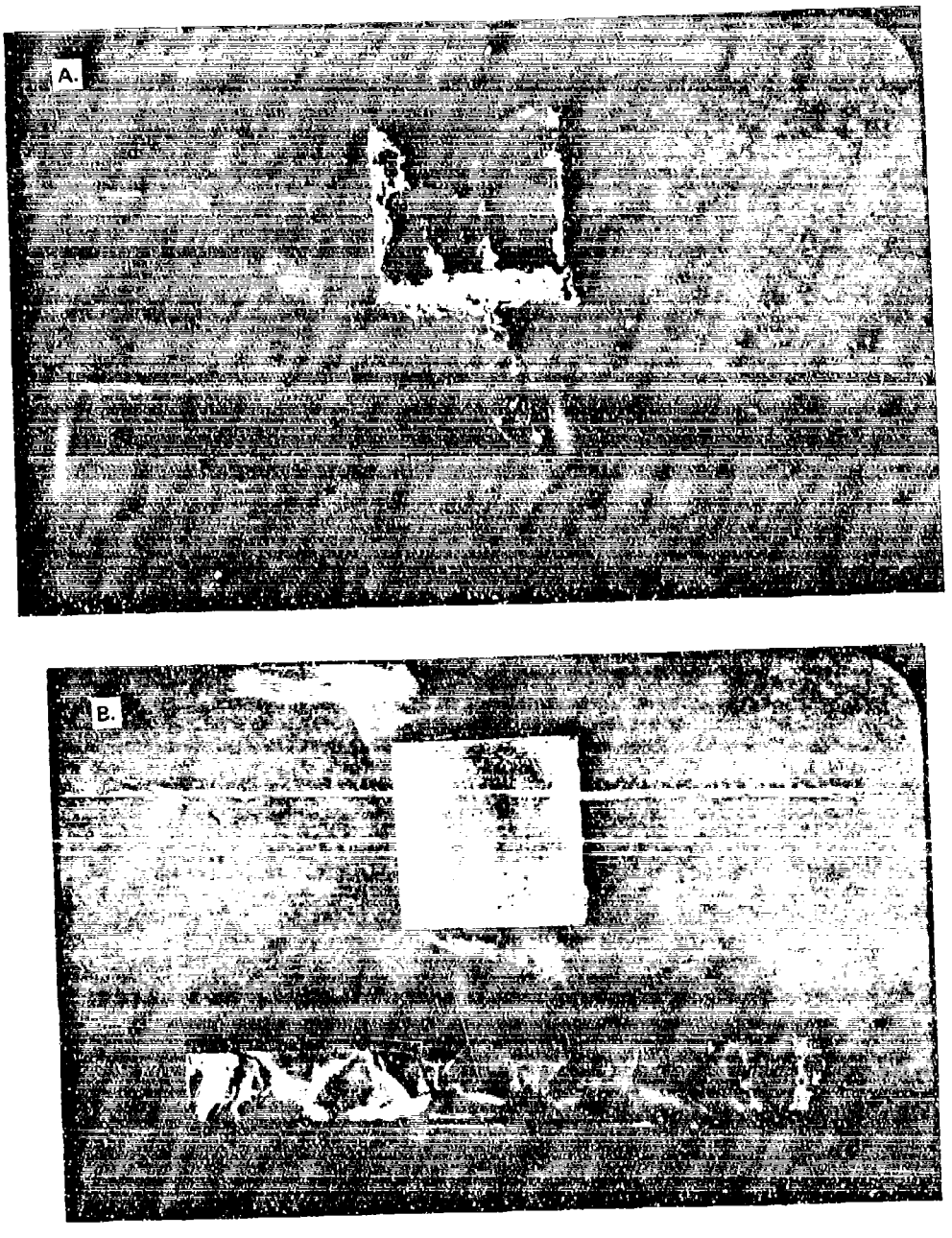

FIGURE 14. PHOTOGRAPHS OF Al 7075/ST-4130 GALVANIC COUPLE AFTER EXPOSURE TO A SALT - FOG ENVIRONMENT FOR 96 HOURS
A - CORROSION PRODUCTS INTACT
B - CORROSION PRODUCTS REMOVED

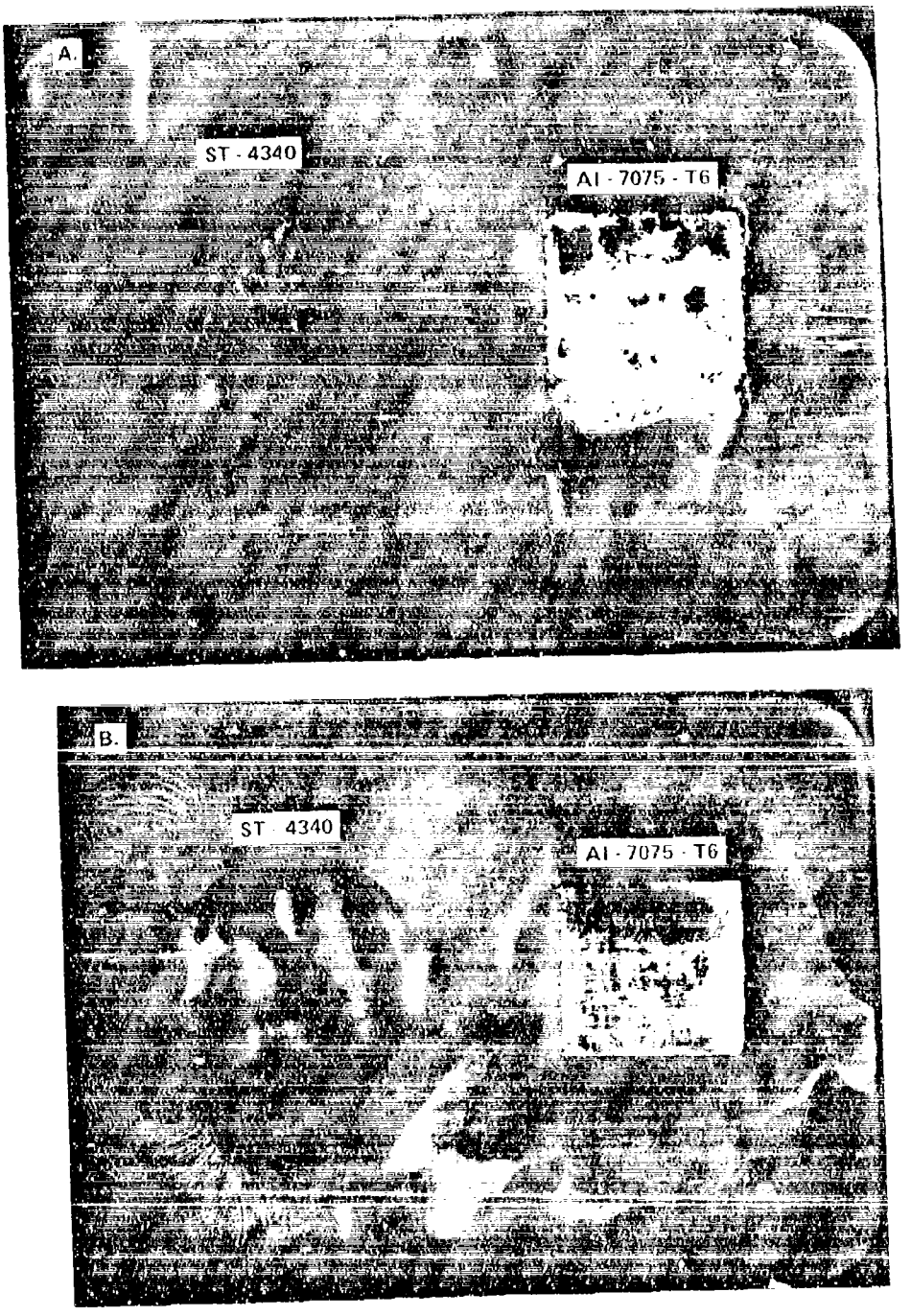

FIGURE 15. PHOTOGRAPHS OF THE Al 7075/STEEL 4340 GALVANIC COUPLE AFTER EXPOSURE TO A SALT FOG ENVIRONMENT FOR 96 HOURS
A - CORROSION PRODUCTS INTACT
B - CORROSION PRODUCTS REMOVED

roughened surfaces were evident. Overall Al-7075 coupled to St-4340 was corroded slightly more than when coupled to St-4130, but not as strongly as when coupled to brass.

Photographs of the St-4340/Brass couple after exposure to the salt-fog environment can be seen in Figure 16. As shown in figure 16A, St-4340 was significantly attacked, similar to that of St-4340 coupled to Al-7075; in this case, St-4340 was more severly attacked, shown in Figure 16B, where the local regions of corrosion product build-up covered deep-roughened areas of uniform attack, about 60% of the metal surface was affected. For brass, surface discoloration was similar to that observed for brass coupled to Al-7075. The surface film was easily removed with a rubber eraser abrasion lines were obvious and, therefore indicated that no measurable corrosion had occurred.

Uncoupled Metal Behavior

The corrosion behavior of the individual metal samples exposed to the salt-fog environment was also investigated in order to make better comparisons to the galvanic couples. Photographs for these samples can be seen in Figures 17 thru 20. The corrosion behavior of Al-7075 shown in Figure 17B, was similar to the Al-7075 samples that were galvanically coupled, that is, the surface was covered with white and black corrosion products; however, once the products had been removed it was noticed that, although the surface was pitted, the pits were extremely small in size and, in addition, a number of areas were uniformly corroded. Uniform attack was not extensive and, in general, the uncoupled Al-7075 was more corrosion resistant than any of the galvanically coupled Al-7075's.

The uncoupled freely corroding brass sample behaved differently from the coupled samples. See Figure 18. Brass had large regions of continuous discoloration and localized regions of blue-green ad pink corrosion products. See Figure 18B. Corrosion products found on uncoupled brass were not as easily removed as those found on coupled brass. Corrosion product removal revealed a surface which had a significant number of pits of irregular shape in concentrated areas, presumably beneath the greenish-blue and pinkish corrosion product regions. See Figure 18C.

Uncoupled St-4340 behavior was similar to coupled St-4340 samples. The metal surface was covered with voluminous yellowish-brown and black corrosion products in somewhat localized areas. See Figures 19A and 19B. Significant corrosion occurred beneath regions of corrosion product build-up in Figure 19C; attack resulted in a roughened surface that was heavily pitted. Areas adjacent to corrosion product build-up showed signs of uniform attack together with some small pits. Approximately 50% of the metal surface was severely corroded.

FIGURE 16. PHOTOGRAPHS OF THE STEEL - 4340/BRASS GALVANIC COUPLE AFTER EXPOSURE TO A SALT - FOG ENVIRONMENT FOR 96 HOURS
A - CORROSION PRODUCTS INTACT
B - CORROSION PRODUCTS REMOVED

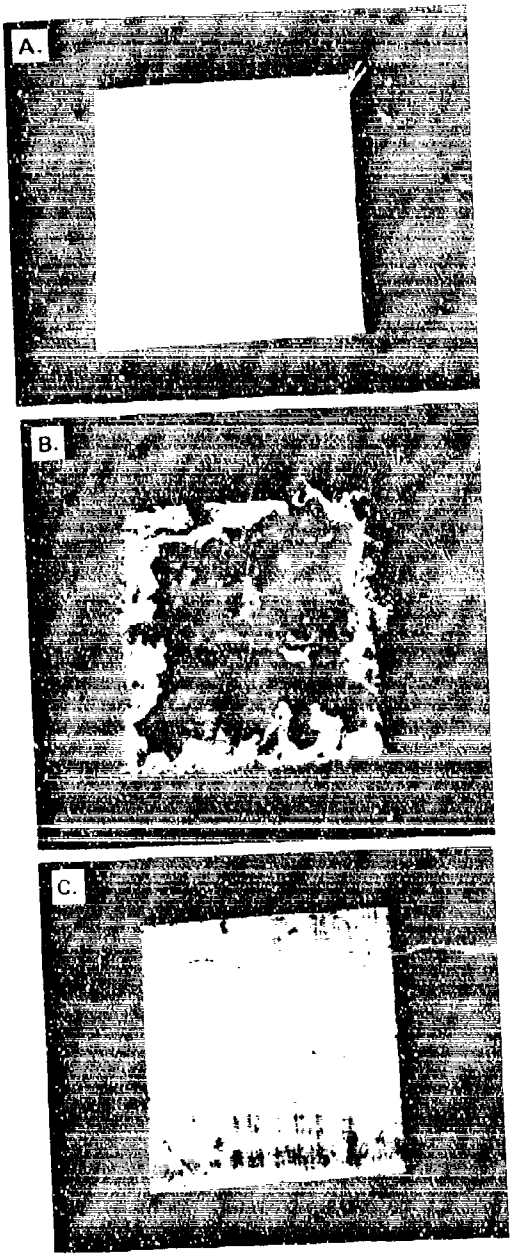

FIGURE 17. PHOTOGRAPHS OF Al-7075-T6 EXPOSED TO SALT - FOG ENVIRONMENT FOR 96 HOURS
A - BEFORE EXPOSURE
AFTER EXPOSURE
B - CORROSION PRODUCTS INTACT
C - CORROSION PRODUCTS REMOVED

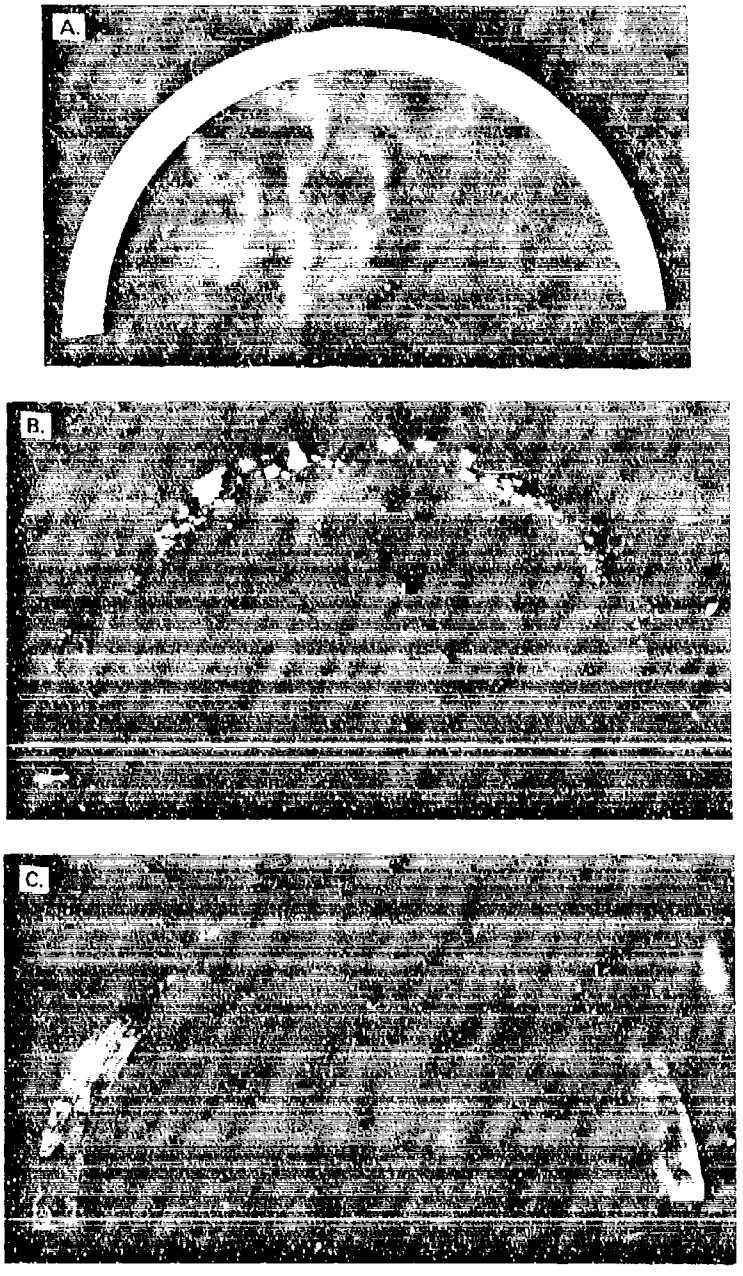

FIGURE 18. PHOTOGRAPHS OF BRASS EXPOSED TO SALT - FOG ENVIRONMENT FOR 96 HOURS
A - BEFORE EXPOSURE
AFTER EXPOSURE
B - CORROSION PRODUCTS INTACT
C - CORROSION PRODUCTS REMOVED

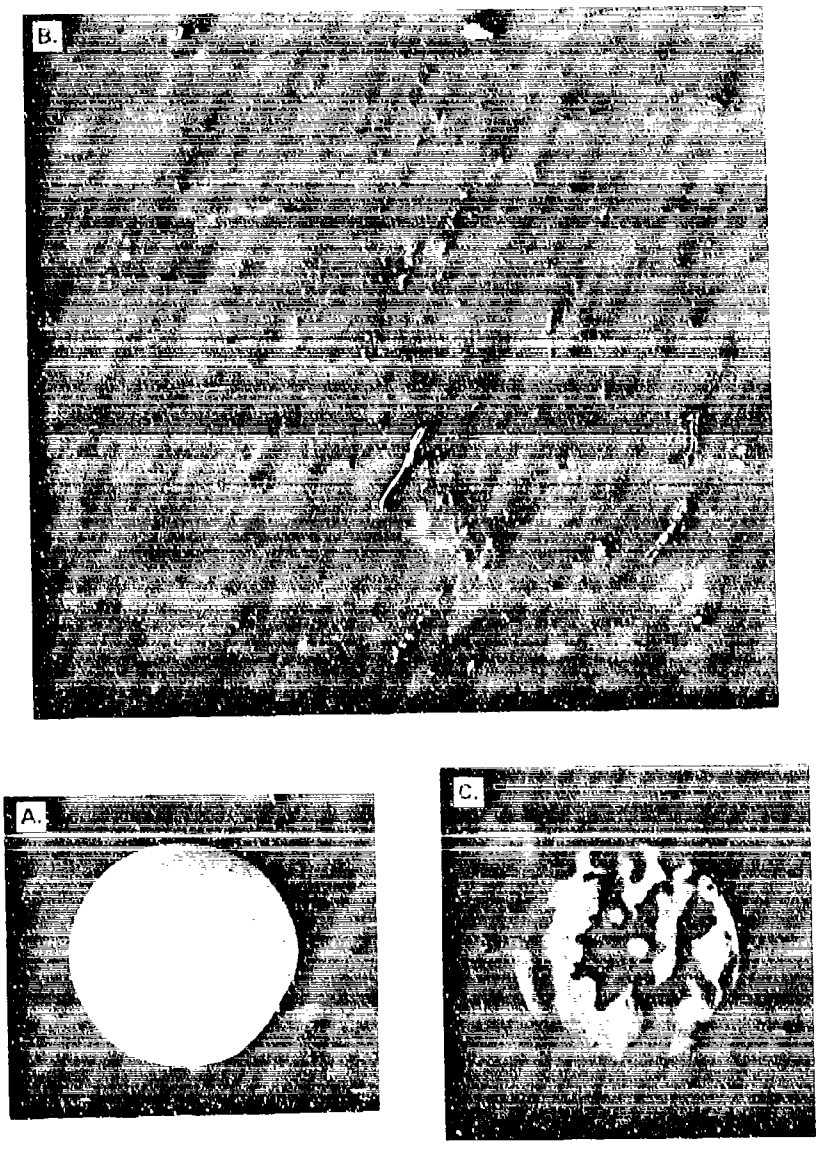

FIGURE 19. PHOTOGRAPHS OF ST-4340 EXPOSED TO SALT-FOG ENVIRONMENT FOR 96 HOURS
A - BEFORE EXPOSURE
AFTER EXPOSURE
B - CORROSION PRODUCTS INTACT
C - CORROSION PRODUCTS REMOVED

Surprisingly the uncoupled St-4130 sample was not corroded as severely as the St-4130 sample coupled to Al-7075 (compare Figures 14A and 20B). However, the smaller regions of corrosion did show signs of increased activity, i.e., deeper more uniform attack, in two closely spaced areas that covered approximately 10-15% of the metal surface. See Figure 20C. These deeply corroded areas were located on the lower-half of the metal in the position of exposure in the salt-fog chamber, i.e., 45 degree angle. A concentrated build-up of liquid and corrosion products in these areas would explain why preferential attack occurred there. Several other regions of less severe uniform attack were found in adjacent areas. In addition, small pits were found randomly dispersed along the metal surface.

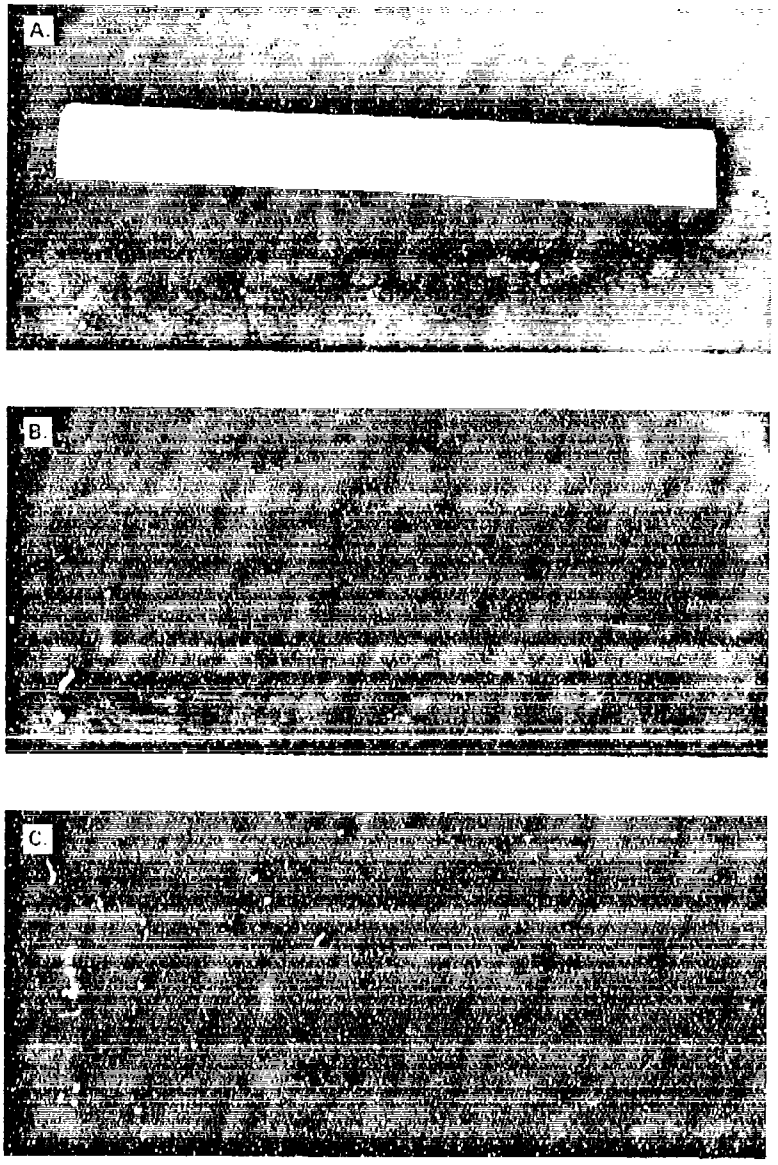

FIGURE 20. PHOTOGRAPHS OF STEEL 4130 EXPOSED TO SALT - FOG ENVIRONMENT FOR 96 HOURS
A - BEFORE EXPOSURE
AFTER EXPOSURE
B - CORROSION PRODUCTS INTACT
C - CORROSION PRODUCTS REMOVED

Chapter 4

THEORETICAL RELATIONSHIP BETWEEN GALVANIC CURRENT AND CORROSION RATE

The magnitude of the galvanic current density generated for different couples is not, in most cases, directly related to the corrosion current density, i.e., corrosion rate. Mansfeld and others (4, 7-9) present theoretical discussions pertaining to the relationship between measured galvanic currents and corrosion rates. Three representative cases, as outlined by Mansfeld (7-9), typical of galvanic behavior will be highlighted below. In the first case, the galvanic couple potential, Ecouple, is far removed from the corrosion potential, Ecorr, of both uncoupled metals. It is assumed that only an oxidation reaction (metal dissolution) occurs at the anode and only a reduction reaction occurs at the cathode. The measured galvanic current, Ig, will equal the dissolution current, I_d^a, for the anode of the couple provided the individual anodic and cathodic reactions exhibit Tafel behavior under charge transfer control:

$$I_g = I_d^a \tag{2}$$

Corrosion of galvanic couples exposed to neutral aerated solutions are strongly influenced by diffusional control, i.e., the limiting current density for oxygen diffusion. For the second case, it is assumed that the only reaction occurring at the cathode is the reduction of oxygen; in addition, it is assumed that both anodic and cathodic reactions occur at the anode. However, the individual rates for oxygen reduction at the anode and cathode are considered to be unequal; this assumption must be true because diffusional control will strongly influence the galvanic current and if by chance the rate of oxygen reduction were equal for all metals, a dependence on the nature of the metal cathode would not be observed. As a result, the anodic dissolution current, I_d^a, for the anode in the galvanic couple must be equal to the sum of reduction currents at the anode, I_c^a, and cathode, I_c^c:

$$I_d^a = I_c^a + I_c^c \tag{3}$$

From Equation (3) it follows:

$$i_d^a A^a = i_c^a A^a + i_c^c A^c \tag{4a}$$

$$i_d^a = i_c^a + i_c^c \tag{4b}$$

where A^a and A^c are the surface areas for the anode and cathode. From Equation (4b), the dissolution current density for the anode, i_d^a, is equal to the sum of the cathodic current densities at the anode and cathode for equivalent surface areas. For a diffusion controlled process, the measured galvanic current density will be equal to the limiting diffusion current density for oxygen reduction at the cathode:

$$i_g = i^c_{L,O_2} = i^c_c \tag{5}$$

where i^c_{L,O_2} is the limiting diffusion current density for oxygen reduction at the cathode. For the uncoupled anode, it is assumed that the cathodic current density is determined by the limiting diffusion current density and, as a consequence, can be taken to be equivalent to the corrosion current density:

$$i^a_c = i^a_{L,O_2} = i^a_{corr} \tag{6}$$

where i^a_{L,O_2} is the limiting diffusion current density for oxygen reduction at the anode and i^a_{corr} is the uncoupled corrosion rate for the anode. Since it is assumed that Equations (5) and (4b) are valid, the galvanic current density is, therefore, equal to the difference between the oxidation current densities, i^a_a, and the reduction current densities, i^a_c, of the anode at Ecouple:

$$i^c_{L,O_2} = i_g = i^a_a - i^c_c \tag{7}$$

Rearranging Equation (7) and substituting with Equation (6):

$$i^a_a = i^a_d = i_g + i^a_c \tag{8a}$$

$$i^a_d = i_g + i^a_{L,O_2} \tag{8b}$$

$$i^a_d = i_g + i^a_{corr} \tag{8c}$$

Equations (8b) and (8c) arise from the assumption that reactions occurring at the anode can be described by Equation (6). Therefore, the dissolution current density for the anode in a galvanic couple is equal to the sum of the measured galvanic current density and the corrosion current density for the uncoupled anode, Equation (8c).

For case III, Ecouple is located so near to Ecorr of the uncoupled anode that both anodic as well as cathodic reactions occur at an appreciable rate at the anode and, as a consequence, Tafel behavior is not exhibited for the dissolution reacton at the anode. It is then observed that the dissolution current will fall between:

$$I_g \leq I_d^a \leq I_g + Icorr \qquad (9)$$

where Icorr is the corrosion current of the uncoupled anode.

In order to compare the theoretical expressions to experimental results for this galvanic study, it is necessary to relate Polarization Resistance (Rp) values to corrosion current densities. It's important to introduce this material at this time so calculated rates of corrosion can be compared to experimental values determined using the Rp technique. Equation (1) given below relates the corrosion current density to the measured Rp value:

$$i_{corr} = 1/\ Rp \cdot \frac{\beta a \beta c}{2.303(\beta a + \beta c)}$$

According to Stern (10), for a diffusion controlled process where Bc $= \infty$, the following form of Equation (1) should be used:

$$i_{corr} = \beta a/2.303 \cdot 1/Rp \qquad (10)$$

Thus, provided a reasonable value for βa is available from either separate experiments or reported literature values, the corrosion current density can be calculated. Measured values of βa for Al-7075, St-4130, and St-4340 are given in Table 7 along with the corresponding corrosion current densities calculated using Equation (10). The values in Table 7 appear to be reasonably accurate; for example, i_{corr} determinations for Al-7075 using cathodic polarization curves gave an i_{corr} value of approximately 3.0 $\mu A/cm^2$, a value identical to that listed in Table 7.

For this galvanic study, it is assumed that the cathodic reduction of oxygen was under diffusional control. This assumption was supported by the shapes of the cathodic polarization curves observed for uncoupled samples. See Figure 12. According to Mansfeld's derivations (7-9), the measured galvanic current density, i_g, should be equal to the limiting diffusion current density, i^c_{L,O_2}, for the cathode, see Equation (5). Table 8 compares i^c_{L,O_2} values for uncoupled metals and the generated galvanic current densities for the various couples. The i^c_{L,O_2} values were reasonably close to the i_g values. Differences between i^c_{L,O_2} and i_g observed for St-4130 and St-4340 coupled to Al-7075 can be attributed to the fact that cathodic reactions are not the only reactions occuring on the steel surfaces. In fact, it's obvious from visual inspection as well as from Rp measurements that small dissolution currents were also generated at the steel cathodes when coupled to Al-7075.

TABLE 7. ANODIC TAFEL CONSTANTS AND CORROSION CURRENT DENSITIES FOR UNCOUPLED Al-7075-T6, St-4130 AND St-4340 EXPOSED TO 3.5% NaCl

SAMPLE	βa(mV/decade)	Rp(ohms.cm^2)	i_{corr}(μA/cm^2)
Al-7075	65	9440	2.98
St-4130	110	2160	22.10
St-4340	115	2094	23.80

TABLE 8. CATHODIC LIMITING DIFFUSION CURRENT DENSITY FOR UNCOUPLED METAL SAMPLES AND MEASURED GALVANIC CURRENT DENSITIES FOR SEVERAL COUPLES

UNCOUPLED SAMPLE	$i_{L,O2}$(A/cm^2)	GALVANIC COUPLE	i_g(A/cm^2)
Brass	18.0 ± 1.0	Al-7075/Brass	15.06
		St-4340/Brass	11.47
St-4130	27.0 ± 2.0	Al-7075/St-4130	20.19
St-4340	20.0 ± 0.2	Al-7075/St-4340	14.27
Al-7075	3.0 ± 0.9	*****	***

Al-7075-T6/BRASS GALVANIC COUPLE

The observed galvanic behavior for this couple can be described by Case II and the following list summarizes the conditions and assumptions that are applicable.

1. Ecouple is far removed from Ecorr of brass, ca., -516 mV.
2. Ecouple is near Ecorr of Al-7075, ca., 48 mV, in the region of mixed-potentials.
3. Cathodic reaction is under diffusional control.
4. Only oxygen reduction occurs at brass-cathode.
5. Rates of oxygen reduction on brass and Al-7075 are not equal.
6. Al-7075 supports both anodic dissolution and the cathodic reduction of oxygen.

The primary concern for this study is to predict the accelerated corrosion rate for an anodic material in a given galvanic couple. For Al-7075/Brass, the dissolution current density, i_d^a, for Al-7075 can be determined by substitution of the measured values for i_g and i_{corr} into Equation (8c), a calculated value of 18.06 $\mu A/cm^2$ is obtained. The measured Rp value for Al-7075 (See Table 5) is 3,595 ohms.cm^2. Substituting the calculated i_d^a value into Stern's equation, (10), gives a calculated Rp value of 1,570 ohms.cm^2. Comparison of the experimental and calculated Rp values for Al-7075 are, in general, in close agreement.*

STEEL-4340/BRASS GALVANIC COUPLE

The galvanic behavior exhibited by St-4340/Brass is similar to that observed for the Al-7075/Brass couple and is best described by Case II. It is assumed that conditions that applied for the treatment of the Al-7075/Brass couple also hold true for this couple. Using Equation (8c) and making the appropriate substitutions for the measured values of i_g and i_{corr} for the couple and St-4340 respectively gives a dissolution current density, i_d^a, for St-4340 of 31.47 $\mu A/cm^2$. The experimental Rp value obtained for St-4340 (See Table 5) is 1,930 ohms.cm^2 and by using Equation (10) with appropriate substitutions a calculated Rp value of 1,590 ohms.cm^2 is obtained. In this case, a better agreement is observed between measured and calculated Rp values.

---

* It must be noted that it's difficult to use the "Rp" technique to uniquely determine a corrosion rate for Al-7075 because of aluminum's tendency to pit rather than uniformly corrode. This may explain why some discrepancies are observed between calculated and experimentally determined Rp values.

Al-7075/STEEL-4130 and Al-7075/STEEL-4340 GALVANIC COUPLES

The observed galvanic behavior for these couples do not fall into the three cases described earlier as cited from Mansfeld and others (7-9). A new treatment is needed to explain experimental observations. In summary, evidence suggests that St-4130 and St-4340 both support anodic dissolution currents, albeit, small currents, as well as the cathodic reduction of oxygen. With this in mind, the conditions and assumptions that best describe the experimental behavior for both aluminum-steel couples is as follows:

1. Reduction of oxygen is under diffusional control.
2. Ecouple values for St-4130 and St-4340 are near their respective Ecorr values, in the region of mixed-potentials.
3. Given 2., it is assumed that both anodic and cathodic reactions occur at the steel cathodes.
4. Ecouple for Al-7075 is located in the Tafel region for anodic dissolution.
5. Ecouple of Al-7075 is far enough removed from Ecorr so that only anodic dissolution occurs on Aluminum.

Since only anodic dissolution occurs on Al-7075 and Ecouple is located in the anodic Tafel region, the dissolution current density, i_d^a, for Al-7075 is taken to be equal to the measured galvanic current density:

$$I_g = I_d^a \tag{11}$$

Furthermore, at Ecouple, the galvanic current at the anode and cathode must be equal:

$$I_g^a = I_g = I_g^c \tag{12}$$

Following the same line of reasoning as used for the development of Equation (7):

$$i_d^a = i_g = i_{L,O_2}^c - i_d^c \tag{13}$$

where i_d^c is the current density due to anodic dissolution at the cathode, i.e., St-4130 or St-4340, i_g is the measured galvanic current density and i_{L,O_2}^c is the limiting diffusion current density for oxygen reduction at the cathode. Rearranging Equation (13) gives the following:

$$i_d^c = i_{L,O_2}^c - i_g \tag{14}$$

For example, an i_g value of 20.19 $\mu A/cm^2$ was obtained for the Al-7075/St-4130 couple. Assuming that Equation (11) is valid, the dissolution current density for Al-7075 is then equal to 20.19 $\mu A/cm^2$ and substitution of this value into

Equation (10) gives a calculated Rp value of 1,400 ohms.cm^2 as compared to the experimental value of 2,500 ohms.cm^2. On the other hand, substituting the appropriate values into Equation (14) results in a dissolution current density density, i_d^c, for St-4130 of 7.0 μA/cm^2. This value of i_d^c translated into a calculated Rp value of 6,823 ohms.cm^2 (a higher Rp value than observed for the uncoupled St-4130 as would be expected, as seen in Table 2) as compared to the measured value of 1,730 ohms.cm^2. This discrepancy can be explain as follows; Rp measurements are obtained after the galvanic couple is disconnected and the individual samples are allowed to reach their respective Ecorr value, this alone will lower the observed Rp value below what one might expect for the coupled state and, therefore, it must be assumed that two, perhaps synergistic, effects are acting on the St-4130 sample after de-coupling. It is proposed that the following equations apply:

$$i_{tot} = i_{corr}^c + i_d^c \tag{15a}$$

$$i_{tot} = i_{L,O_2}^c + i_d^c \tag{15b}$$

where i_{tot} is corrosion current density that results as a consequence of de-coupling and equilibration at Ecorr and is equal to the sum of the limiting diffusion current density for uncoupled St-4130, i.e., the corrosion rate for the uncoupled metal, and the dissolution current density of coupled St-4130 obtained from Equation (14). Substitution of appropriate values in Equation (15b) gives an i_{tot} value of 34.0 μA/cm^2 which, after substitution into Equation (10), gives a calculated Rp value of 1,400 ohms.cm^2. The calculated Rp value is a good approximation of the measured Rp value of 1,730 ohms.cm^2. Therefore, it must be noted that caution must be exercised when using the Polarization Resistance Technique to predict the corrosion rate of galvanically coupled metals, although, Rp values do show general trends for corrosion rates of galvanic couples.

For St-4340, an i_d^c value of 5.73 μA/cm^2 is calculated using Equation (14), which gives an Rp value of 8,700 ohms.cm^2 as compared to the measured value of 2,450 ohms.cm^2. Application of Equation (15b) gives an i_{tot} value of 25.7 μA/cm^2 which translates into an estimated Rp value of 1,940 ohms.cm^2, a good approximation for the experimentally determined value of 2,450 ohms.cm^2. Again, some discrepancies were found when calculated and experimental Rp values were determined for Al-7075 in the Al-7075/St-4340 couple. Assuming that Equation (11) holds true for this couple, i_d^c equals 14.27 μA/cm^2, which gives a calculated Rp value of 2,000 ohms.cm^2 as compared to the experimentally determined value of 4,950 ohms.cm^2.

CORROSION RATES FOR GALVANIC COUPLES

Corrosion current densities give an indication of the magnitude to which corrosion will occur but no physical significance can be identified with either i_{corr} or i_d values. Typically, corrosion rates ar described in terms of weight lost/area/day, i.e., mg/dm^2/day (m.d.d.), or a number of milli-inches penetrated/year (m.p.y). Calculation of corrosion rates in more meaningful terms can be accomplished by use of the Faraday equation:

$$Q/F = w/E.W. \quad (16a)$$

$$Ixt/F = w/E.W. \quad (16b)$$

Rearranging (16b) gives:

$$w/t = IxE.W./F \quad (17)$$

where Q is the number coulombs, F is the Faraday constant (96,487 coul), w is the weight in grams, E.W. is the equivalent in grams, I is the current in amps, and t is the time in seconds. When the corrosion current density, i_{corr} is substituted for I in Equation (17) and other appropriate substitutions are made Equation (17) takes on the following form, allowing corrosion rates to be represented as "milli-inches per year", m.p.y.:

$$m.p.y. = 0.13 \times i_{corr} \times E.W. / p \quad (18)$$

where i_{corr} is the corrosion current density in $\mu A/cm^2$ and p is the density of the material in g/cm^3. In addition, corrosion rates are commonly represented as $mg/dm^2/day$ (m.d.d.); for this representation, Equation (17) takes on the following form:

$$m.d.d. = 0.0895 \times i_{corr} \times E.W. \quad (19)$$

Table 9 gives a summary of the measured galvanic data and the calculated corrosion rates for the individual metals of each galvanic couple. In addition, the corrosion rates for the uncoupled anodes and cathodes are listed in the last column. Corrosion rates are calcuated using Equation (19). Since brass only supports cathodic reduction currents when galvanically coupled to Al-7075 or St-4340 its corrosion rate should decrease significantly; however, Rp data indicated that the corrosion rate for brass remained unchanged or increased slightly after galvanic measurements were ceased. This observation was reasonable because Rp measurements were obtained for de-coupled samples after some equilibration at Ecorr. From this table, it can be seen that the corrosion rate for Al-7075 doubled from an uncoupled value of 7.2 to 14.5 m.d.d. when coupled to brass, a similar increase was found when coupled to St-4130. The corrosion rate of Al-7075 increased by about 1.5 times when coupled to St-4340. Although the steel samples in this study behaved primarily as cathodes, small corrosion rates were detected; for St-4130, a decrease in the corrosion rate from an uncoupled value of 55.3 m.d.d. to a value of 17.5 m.d.d. occurred when coupled to Al-7075 and, for St-4340, the corrosion rate decreased from an uncoupled value of 59.6 to 14.3 m.d.d. when coupled to Al-7075.

TABLE 9. SUMMARY OF GALVANIC CORROSION DATA

GALVANIC COUPLE	i ($\mu A/cm^2$)	ANODE/ CATHODE	i_d^a or i_d^c ($\mu A/cm^2$)	CORROSION RATE (m.d.d.) COUPLED	UNCOUPLED
Al-7075/Brass	15.06	Al-7075	18.06	14.5	7.20
		Brass	****	****	****
St-4340/Brass	11.47	St-4340	31.47	78.6	59.6
		Brass	****	****	****
Al-7075/St-4130	20.19	Al-7075	20.19	16.2	7.20
		St-4130	7.0	17.5	55.3
Al-7075/St-4340	14.27	Al-7075	14.27	11.48	7.20
		St-4340	5.73	14.30	59.60

CHAPTER 5

CONCLUSIONS

1. The uniform corrosion rate for the uncoupled samples, as measured using the Polarization Resistance Technique, can be arranged in the following order of decreasing corrosion resistance: St-4340 < St-4130 < Brass < Al-7075-T6.

2. Results from immersion studies in 3.5% NaCl indicated that the highest galvanic current density was produced by the Al-7075/St-4130 couple, followed by: Al-7075/Brass, Al-7075/St-4340, St-4340/Brass.

3. In all cases studied, higher galvanic current densities were generated for large cathode-to-anode area ratios. It is suggested that a small cathode-to-anode area ratio be employed when unfavorable metals must be joined.

4. For exposure to 3.5% NaCl, corrosion rate of Al-7075-T6 was significantly accelerated when coupled to Brass, St-4130, and St-4340. The corrosion rate of St-4340 was similarly accelerated in the St-4340/Brass couple. Brass remained the cathode in all galvanic couples and exhibited no tendency to corrode. On the other hand, both St-4130 and St-4340 showed signs of localized attack when coupled to the more anodic Al-7075-T6 alloy.

5. For salt-fog exposure, the corrosion of Al-7075-T6 coupled to Brass and both steels showed signs of extensive pitting and discoloration with a concurrent build-up of white corrosion products. Brass remained unaffected except for some slight discoloration, beneath which no signs of corrosion could be detected. The corrosion rate of St-4340 was accelerated when coupled to Brass and, in addition, a significant amount of corrosion was observed for St-4340 in the Al-7075/St-4340 couple. As observed for St-4340, St-4130 was severely attacked when coupled to Al-7075-T6.

6. Uncoupled Brass exposed to the salt-fog environment revealed severe discoloration with a large number of small pits beneath regions of bright colored corrosion products. Al-7075-T6 showed more resistance to the salt-fog environment in the uncoupled state, revealing only extremely small pits and some uniform corrosion. Uncoupled St-4340 behaved similarly to the coupled samples, pitting was observed in areas adjacent to regions of severe uniform attack. The exposure of St-4130 to a salt-fog revealed a reduction in the area of attack but showed an increase in the depth of penetration in those regions that were corroded.

7. Application of theoretical expressions helped to better explain the nature of the relationship between the measured galvanic current and the corrosion rate of the individual metals in a couple.

8. Experimental as well as theoretical treatments showed that non-negligible anodic reactions occurred at the steel cathodes when galvanically coupled to Al-7075-T6, however, a decrease in the corrosion rate for both St-4340 and St-4130 can be expected when coupling to Al-7075-T6 occurs.

9. A comparison was made between measured Rp values and calculated corrosion rate values. Careful consideration and caution must be exercised when Rp measurements are used to determine corrosion rates for galvanic couples.

REFERENCES

1. Mansfeld, F., and Kenkel, J. V., Ed., Galvanic and Pitting Corrosion-Field and Laboratory Studies (Philadelphia, PA: A.S.T.M., STP 576, 1976), p. 20.

2. Baboian, R., ibid., p. 5.

3. Reboul, M. C., Corrosion, Vol. 35, No. 9, 1979, p. 423.

4. Mansfeld, F., Hengstenberg, D. H., and Kenkel, J. V., Corrosion, Vol. 30, No. 10, 1974, p. 343.

5. Stern, M., and Geary, A. L., J. Electrochem. Soc., Vol. 104, 1957, p. 56.

6 Pryor, M. J., and Kier, D. S., J. Electrochem. Soc., Vol. 102, No. 10, 1955, p. 605.

7. Mansfeld, F., and Parry, E. P., Corr. Sci., Vol. 13, 1973, p. 605.

8. Mansfeld, F., Corrosion, Vol. 27, 1971, p. 436.

9. Mansfeld, F., Corrosion, Vol. 29, 1973, p. 403.

10. Stern, M., Corrosion, Vol. 14, 1958, p. 60.

DISTRIBUTION

	Copies
Office of Naval Research Attn: S. Fishman, Code 1131 800 N. Quincy St. Arlington, VA 22217	2
Office of Deputy Undersecretary of Defense Engineering Staff Specialist for Materials Attn: J. Persh Washington, DC 20301	1
Defense Advanced Research Attn: P. Parrish 1400 Wilson Blvd. Arlington, VA 22209	1
Naval Ocean Systems Command Attn: P.D. Burke, Code 932 San Diego, CA 92152	1
Naval Surface Weapons Center Attn: K. Musselman, Code R35	2
J. Hall, Code R35 Dahlgren, VA 22448	2
Naval Air Development Center Attn: V. Agarwala, Code 6062	2
J. Thompson, Code 6062 Warminster, PA 18974-5000	2
U.S. Bureau of the Mines Attn: C. O'Dell 4900 LaSalle Road Avondale, MD 20782	1
John Hopkins University Dept. of Material Science and Engineering Attn: J. Kruger	1
P. Moran	1
J. Prentice Maryland Hall Baltimore, MD 21218	1
Library of Congress Attn: Gift and Exchange Division Washington, DC 20540	4
Department of the Army Attn: A. Levitt AMMRC DRXMR-MMC, Bldg. 39 Watertown, MA 02172	1
Naval Research Laboratory Attn: R. Crowe, Code 6372	1
E. McCafferty	1
P. Trzaskoma	1
P. Natishan Washington, DC 20375	1
Naval Material Command Office of Naval Technology Attn: J.J. Kelly, Code 0725	1
A.J. Sedrike, Code 431 Washington, DC 20360	1
Defense Technical Information Center Cameron Station Alexandria, VA 22314	12
Naval Sea Systems Command Attn: S. Rodgers, SEA 05M1	1
H. Bliele, SEA 05M1 Washington, DC 20362	1
David Taylor Naval Ship Research and Development Center Attn: T. Morton, Code 2813	1
H. Jack, Code 2813	1
J. Scully, Code 2813	1
D. Aylor, Code 2813 Bethesda, MD 20084	1
Vance Sage PMS 400C52 NC210S18 2521 Jefferson Davis Hwy. Arlington, VA 22202	1
University of Virginia Dept. of Materials Science Attn: G. Stoner	1
G. Cahen Thornton Hall Charlottesville, VA 22901	1

DISTRIBUTION (Cont.)

		Copies
Internal Distribution:		
R33	(J.F. McIntyre)	10
R33	(C.E. Mueller)	1
R33	(D. Warburton)	1
R33	(Staff)	25
R30		2
R32	(S. Hoover)	1
R32	(K. Vasanth)	1
R32	(J. Jarus)	1
R32	(W. Lee)	1
R35	(E.P. Lefeave)	1
E35		1
E231		9
E232		3